Optimization of Line Start Permanent Magnet Synchronous Motor for Magnet Cost Reduction

Amit Kumar Jha

KTH Electrical Engineering

Degree project in
Electrical Machines and Drives

Stockholm, Sweden 2012

XR-EE-E2C 2012:019

KTH Electrical Engineering

Optimization of Line Start Permanent Magnet Synchronous Motor for Magnet Cost Reduction

by

Amit Kumar Jha

Master Thesis

Supervisor :
Dr. Tanja Hedberg
Dr. Öystein Krogen

Examiner :
Prof. Chandur Sadarangani

Royal Institute of Technology
The School of Electrical Engineering
Electrical Energy Conversion
Stockholm, 2012

XR-EE-E2C 2012:019

Abstract

In this thesis different methods of optimizing line start permanent magnet motor (LSPM) for magnet cost reduction is studied. Influence of different parameters has been studied by simulating magneto-static and transient FEM models of the machine. Finally a motor design of a LSPM with high rotor saliency has been proposed.

The first method investigated is the use of flux barriers in LSPM and its effect on the magnetic flux leakage. The flux barriers reduce the flux leakage and hence help in reducing magnet volume. The second method studied is the use of two different grades of magnets. Using low price magnets help in reducing the total magnet cost without reducing the air gap flux density. The reduction in NdFeB magnet volume is not substantial by using both the methods mentioned above.

The third method investigated is increasing the saliency of the rotor by introducing flux barriers and reducing the corresponding magnet volume. Both the magneto static and transient models are used to study the effect of different parameters of the motor. The placement and volume of magnet plays a critical role in motor performance. At first, the developed reluctance torque of the motor is maximized by doing parametric study and then magnets are placed in slots to achieve the required efficiency and power factor. The motor is simulated with NdFeB magnets and with Ferrite magnets. It has been found that using high saliency LSPM motor the NdFeB magnet volume can be reduced significantly. It is also shown that the same performance of motor (as compared to the motor with NdFeB magnets) can be achieved by using Ferrite magnets. The volume of Ferrite magnet required will be larger but still cost-wise using Ferrite is an attractive choice. Therefore, a design of motor is proposed using both NdFeB magnets and Ferrite magnets. Finally, the performance of proposed LSPM motor with high saliency is compared with that of an induction motor.

Index Terms: Line start reluctance motor, LSPM, magnet assisted reluctance motor, Magnet volume reduction, Optimization of LSPM.

Sammanfattning

I denna thesis har olika metoder för att optimera Line Start Permanent Magnet Motor (LSPM) mrd avseende på magnetkostnad. Påverkan av olika parametrar har studerats genom simuleringar av magnetostatiska och transienta beräkningar. Dessa studier genomfördes på finiteelementbaserade modeller. Slutligen har en design av LSPM med hög rotor saliency tagits fram.

Den första undersökta metoden är användningen av flödesbarriär i LSPM och dess effekt på det magnetiska läckflödet. Flödesbarriärer minskar läckflödet och bidrar därmed till att minska magnetvolymen. Den andra metoden som studeras är användandet av två olika magnetmaterial som används. Genom att använda den billigare magnetmaterial minskas den totala magnetkostnaden medan flödestätheten i luftgapet blir oförändrad. Användning av båda metoderna som nämns ovan är inte betydande gällande mängden av NdFeB-magnet.

I den tredje metoden ökas rotor saliency genom att introducera flödesbarriärer och reducera motsvarande magnetmängd. Både magneto-statiska och transienta modeller används för parameterstudien. Magnetplaceringen och magnetvolymen spelar en kritisk roll i motorprestanda. Till en början är den delen av vridmomentet som orsakas av reluktansen i rotorn som maximeras genom en parameterstudie och därefter placeras magneter i spåren för att uppnå önskad verkningsgrad och effektfaktor. Simuleringarna görs med NdFeB-magneter och Ferrite-magneter. Det har visat att LSPM motorer med hög saliency minskar volymen av NdFeB magneter avsevärt. Det visas också att samma prestanda hos motorn (jämfört med motorn med NdFeB-magneter) kan uppnås genom att använda Ferritmagneter. Det krävs en större volym av Ferritmagneter men prismässigt är ferrit ett attraktivt val. Därför föreslås en motorkonstruktion som innehåller både NdFeB och Ferritmagneter. Slutligen är den föreslagna LSPMmotorns prestanda jämförbar med en asynkronmotor.

Sökord: Line start reluctance motor, LSPM, magnet assisted reluctance motor, Magnet volume reduction

Acknowledgment

This master thesis has been done at the department of Research and Development, Xylem in Stockholm, Sweden and I am thankful to Xylem for offering this master thesis to me.

I am deeply thankful to my supervisor Dr. Tanja Hedberg for all the support and guidance during the thesis work and for correcting the final report. I am also thankful to Dr. Öystein Krogen for the valuable suggestions in the thesis work and for the suggestions to improve the report.

I am grateful to Prof. Chandur Sadarangani for invaluable discussions and examining my thesis work. I am also thankful to Prof. Juliette Soulard for introducing me to Xylem for thesis work. I am deeply thankful to Kashif Saeed khan for valuable discussion and suggestion which helped me a lot in completing the work.

I would also like to extend my gratitude to Karl Hultqvist and Zhiyong Zhong for all the discussions and constructive comments. I also thank Mila Naghibian for reviewing my report. It has been a pleasure to work in the friendly environment.

I am grateful to my parents for their encouragement as well as financial support to continue education. Special thanks to my brothers Rajeev Jha and Ashish Jha who have always inspired and guided me to achieve the desired goals.

Finally, I would like to appreciate my friends,Sneha Singh and Hitesh Pandey for their support and encouragement during the thesis work.

Amit Kumar Jha
Stockholm , Sweden
Date. December 3, 2012

Contents

Abstract iii

Acknowledgement vii

Contents ix

1. Introduction 1
- 1.1. History and Background . . . 1
- 1.2. Basic Operation of LSPM . . . 1
- 1.3. Advantage and Disadvantage of LSPM . . . 2
- 1.4. Thesis objectives . . . 3
- 1.5. Thesis outline . . . 4

2. Operation of LSPM 5
- 2.1. Transient operation . . . 5
  - 2.1.1. Braking torque in LSPM . . . 5
  - 2.1.2. Effect of rotor position at start . . . 7
- 2.2. Steady State operation . . . 8
  - 2.2.1. Synchronization of LSPM . . . 8
  - 2.2.2. Synchronous Torque . . . 12

3. Use of Flux Barrier and Two different grade Magnets 15
- 3.1. Flux Barrier . . . 16
- 3.2. Use of two different grades of magnets . . . 19
  - 3.2.1. Using NdFeB and SmCo magnets . . . 20
  - 3.2.2. Using NdFeB and Ferrite magnets . . . 21
- 3.3. Summary . . . 23

4. LSPM with high saliency 25
- 4.1. Basic working of synchronous reluctance motor . . . 25
- 4.2. Parametric Study . . . 27
  - 4.2.1. Number of barriers . . . 27
  - 4.2.2. Insulation ratio . . . 30
  - 4.2.3. Effect of air gap length . . . 31
  - 4.2.4. Influence of magnet addition . . . 32
  - 4.2.5. Length of Magnet . . . 35
  - 4.2.6. Arrangement of Magnets . . . 36

4.2.7. Stator coil turns 38
4.2.8. Effect of supply voltage 38
4.3. Proposed Design 39
4.4. Summary 44

5. Conclusion and Future Work **47**
5.1. Future Work 49
Appendix

A. Dimensional and performance details of LSPM **51**

Bibliography **53**

List of Figures

1.1. Variation of price of Nd and Dy metal [1] 2
1.2. Cross section of different line start motors 3

2.1. Asynchronous cage torque with magnets and without magnets in LSPM [2] 6
2.2. Flux vectors position for optimal and worst condition for the start . 7
2.3. Synchronous torque variation with load angle 9
2.4. Synchronization of PM motor with Inertia and torque [3] 11
2.5. Variation of maximum power factor with saliency for a purely reluctance motor(no magnets)[4] 12
2.6. Variation of synchronous torque,reluctance torque and flux alignment torque with load angle 13
2.7. Effect of saliency on synchronous torque 14
2.8. Synchronous torque for different magnet volume and saliency 14

3.1. Cross section of LSPM 15
3.2. Magnetic flux lines distribution in LSPM. 16
3.3. Air gap flux density in LSPM 17
3.4. Flux lines distribution with trapezoidal flux barrier 17
3.5. Trapezoidal flux barrier geometry 18
3.6. Effect of trapezoidal flux barrier on air gap flux density 18
3.7. Magnet arrangement of two different grades 20
3.8. Magnet arrangement with Ferrite and NdFeB magnets 22

4.1. Rotor geometry with barriers showing dq axis of the motor 26
4.2. Flux lines distribution due to stator excitation only 27
4.3. Rotor geometry with different number of barriers with equal total width of barrier 28
4.4. Rotor geometry with barriers rearranged 29
4.5. Transient response of geometry 1,geometry 2,geometry 3 under load 29
4.6. Cross section of rotor showing different parameters 30
4.7. Transient response of reluctance motor with different air gap length 32
4.8. Motor geometry with magnet placed in barriers 33
4.9. Variation in efficiency and power factor of geometry 2 35
4.10. Transient response of geometry 2 at rated load with different volumes of magnet 35

4.11. Comparison of L_d/L_q of the rotor with increased and normal magnet length 36
4.12. Same volume of magnet arranged differently in slots 37
4.13. Speed response geometry 2(air gap=0.5mm) with 360 V(line to line) 39
4.14. Cross Section of final design with 40% NdFeB and 107% of Ferrite magnet as compared to magnet volume used in LSPM motors . . . 40
4.15. Comparison between transient behaviour of LSPM and proposed motor (LSPM with high saliency) 40
4.16. Transient speed response of LSPM and the proposed motor at different rotor position at start 41

A.1. Cross section of a pole of LSPM 51

List of Tables

3.1. Flux density variation with length of air at top of magnet(I_top) with A_l=1.5mm,A_w=2.5 19
3.2. Air gap flux density using SmCo and NdFeB magnets 20
3.3. Air gap flux density using Ferrite and NdFeB magnets 21
3.4. Air gap flux density at different volume of ferrite magnet(keeping magnet length fixed F_l =3mm, NdFeB magnets length(Lm2,Lm4) is 22.8mm and Lm3=25.8mm) 22
3.5. Air gap flux density at different volume of ferrite magnet(keeping magnet width fixed F_w=3mm) 22
3.6. Air gap flux density at different volume of ferrite and NdFeB magnets with barrier dimensions are A_w=4.5mm,A_l=1.7mm , I_top = 0.2mm 23

4.1. Change in d and q axis flux with number of flux barriers 28
4.2. Variation of reluctance torque with insulation ratio(kq_{ins}) 30
4.3. Effect of air gap length on performance of machine (geometry 2) . . 31
4.4. The d and q axis flux density at different magnet (NdFeB) volumes . 33
4.5. The d and q axis flux density at different magnet(Ferrite) volumes . 34
4.6. Performance of motor with different magnet arrangements keeping magnet volume constant (40%), calculation of efficiency does not include stray loss 37
4.7. Effect of number of turns on motor performance 38
4.8. Summary of results for 12.5 kW *Magnets used is NdFeB,IM=Induction motor,RM=Reluctance motor,Magnet % used is compared to LSPM* 43
4.9. Summary of results for 11 kW *Magnets used is NdFeB,IM=Induction motor,RM=Reluctance motor,Magnet % used is compared to LSPM* 44

A.1. Dimensional and Performance details of 12.5 kW LSPM 52

Chapter 1

1 Introduction

1.1. History and Background

Line start permanent magnet synchronous motor(LSPM) is a hybrid motor. It exhibits the properties of induction motor in transient state and synchronous motor in steady state. Due to the presence of magnet in the motor LSPM performs at higher efficiency and better power factor compared to the same size induction motor. The idea of LSPM first came around 1950-1960. The magnetic material available at that time was not good enough to make the motor competitive to the induction motor. In early 1980's with the improvement of Neodymium Iron Boron magnets(NdFeB) at low cost made LSPM an attractive choice [5]. NdFeB posses high remanent flux and high coercivity than other magnetic materials. In LSPM magnet quality and cost decides the performance and price of the motor respectively.

In recent years the price of magnets have shown high fluctuations because of the global demands. The price of NdFeB magnet has increased many-fold because of increase in price of its main component Neodymium(Nd). Also the price of dysprosium(Dy) has increased which improves the coercivity of magnet. The variation in price of Neodymium and Dysprosium is shown in figure 1.1 [1]. From the figure, it can be seen that the price of Neodymium has increased rapidly in 2011, which in turn increased the price of NdFeB magnets. Although in 2012 the price of Nd and Dy metal has decreased still it is more than thrice the price during 2009. With the increase in price of magnet the motor will also become costly. To make the LSPM motor competitive in terms of cost the use of magnets has to be minimized without compromising the performance of the motor.

1.2. Basic Operation of LSPM

LSPM have properties of both an asynchronous motor and a synchronous motor. LSPM operates like a permanent magnet synchronous motor(PMSM) in its steady

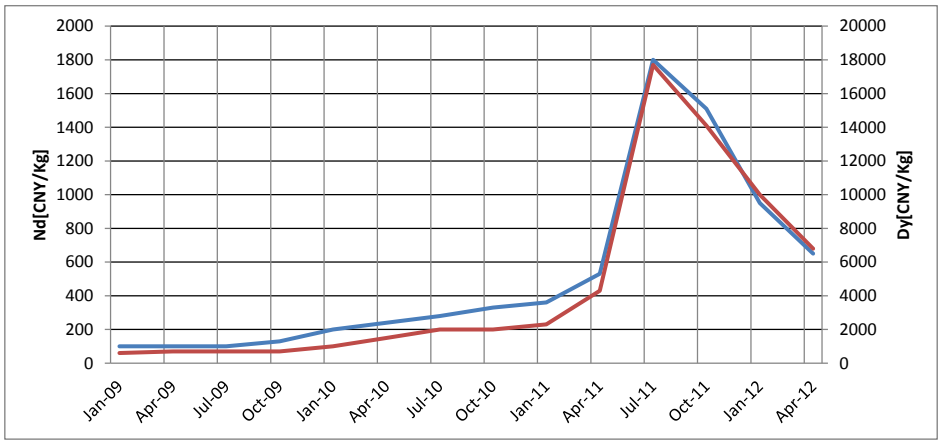

Figure 1.1.: Variation of price of Nd and Dy metal [1]

state. PMSM cannot operate at any speed other than synchronous speed and hence require a drive system to operate. Unlike PMSM, LSPM does not need any drive system. It starts directly on main supply and hence needs rotor bars to start. When three phase supply is applied to the stator coil, it creates a rotating magnetic field. Because of rotating magnetic field current is induced in rotor bars. This current interacts with the field and produces torque to start the motor. Once it reaches the synchronous speed the motor operates like a synchronous motor.

Figure 1.2 shows cross section of different line start motors. The squirrel cage is common in all three motor. The motors behaviour depend on the flux alignment torque (magnet volume) and reluctance torque(saliency of rotor). LSPM has low reluctance torque and high flux alignment torque whereas the motor as shown in figure 1.2(c) will have only reluctance torque(no flux alignment torque).The motor cross section shown in figure 1.2(b) is a hybrid of LSPM and LSRM. The motor will have both reluctance and flux alignment torque.

1.3. Advantage and Disadvantage of LSPM

As LSPM operates like a PMSM in steady state, it has all the advantages of a PMSM. As the motor operates at synchronous speed, theoretically it will not have any rotor current. With no rotor loss the efficiency of the motor will be higher and the operating temperature of the motor will be lower than an induction motor of the same size.

The LSPM has high power factor around 0.9-1 [5], as the magnets in the motor are mainly responsible for the air gap flux. This reduces the stator current required for

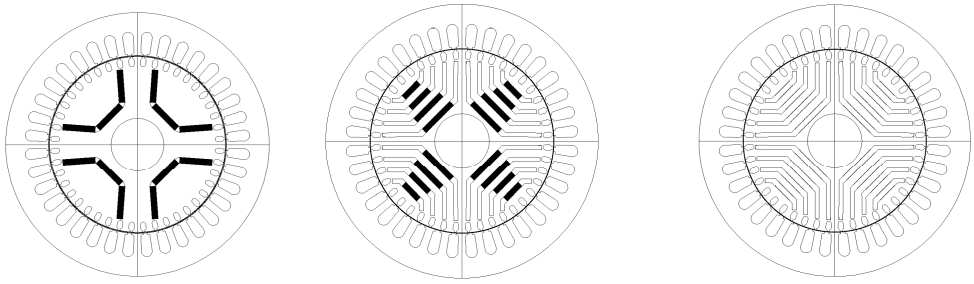

(a) LSPM (b) LSPM with high saliency(LSPM-RM) (c) LSRM (no magnets)

Figure 1.2.: Cross section of different line start motors

the magnetization. The reduction in stator current results in lower stator copper loss and improves the efficiency further. Also the air gap in LSPM is generally larger which helps in reducing the stray load losses and harmonic losses.

The disadvantage of the LSPM is that it is more expensive than the induction motor of the same rating. The price of the motor depends on the price of magnet. The inflation in magnet price in recent years, shown in section 1.1, makes the motor costly.

The LSPM is a hybrid of asynchronous and synchronous motor,which make the design as well as the operation of LSPM complicated. The motor starts as an asynchronous motor and hence should be designed such that it starts directly on main supply. As the motor operates as a synchronous motor at steady state it must also have the required synchronous torque. If the motor is designed with high synchronous torque it might not be able to start and on the contrary if the motor is designed with high asynchronous torque it might not synchronize. Hence there should be compromise between the two torques.

The motor has the same starting torque as compared to the induction motor. But the average transient torque of the LSPM is lower than the induction motor due to the braking torque of the magnet. In transient operation of LSPM the magnets cause very high oscillating transient torque which may damage the mechanical system.

1.4. Thesis objectives

The goal of this thesis work is to reduce magnet volume used in the LSPM which will reduce the cost of the motor.The dimension and performance data is given in appendix A. The different ideas for achieving the goal are as follows:

- **Introduction of flux barriers :** There is leakage of flux created by magnets. This leakage flux does not contribute to the torque production. Hence the magnets where leakage taking place are not useful. This leakage can be reduced by introducing flux barriers (air) which in turn reduces the magnet volume.
- **Use of different grades of magnet :** All parts of the magnet are not subjected to the same demagnetization. Also all parts of magnetic flux does not add uniformly in air gap flux. So, using two different grades of magnets i.e. NdFeB and Ferrite according to the requirement can help in reducing the cost of the magnet in the motor [6].
- **Increasing saliency of the rotor:** The synchronous torque consists of two parts. The first torque is because of the non-alignment of the stator and rotor flux. The developed torque depends on the magnetic flux from the magnet. The second torque is because of the saliency of the rotor. The difference in reluctance cause distortion in the flux and develops torque. The torque depends on the saliency of the rotor. If the second torque is increased then the torque because of the magnet can be reduced. Hence the magnet volume can also be reduced.

1.5. Thesis outline

In chapter 2, the working principle of LSPM is discussed. The different torques and their role in the function of the motor is also presented. The synchronization of LSPM is the final operation and very important to achieve. The parameters which play an important role in synchronizing the motor has also been discussed in the chapter.

In chapter 3, the effect of introducing flux barriers and using different grades of magnet are discussed. The results of the FEM simulation are also presented and discussed.

In chapter 4, the idea of increasing the reluctance torque component in LSPM is discussed in detail. Based on the results from the FEM simulation the role of different parameters in the performance of the motor are presented. The effect of magnet addition in motor with high reluctance torque is also presented. Finally the final design is proposed and its performance is compared with the induction motor of same output power.

In chapter 5, conclusions and proposals for future work are presented.

Chapter 2
2 Operation of LSPM

In chapter 1.2 basic operation of LSPM is described. As mentioned LSPM works on the principle of asynchronous as well as synchronous motor. The operation of the motor is divided into two parts. One, where the motor operates as an asynchronous motor i.e. transient state .The second, where the motor operate as a synchronous motor i.e steady state.

2.1. Transient operation

In transient (during starting)operation the motor behaves asynchronously. The LSPM motor has squirrel cage similar to an induction motor. When the motor is supplied with three phase balanced supply, it generates a rotating magnetic field which induces emf in the cage. As the cage is short-circuited by end-rings, rotor current will flow in the cage bars. The currents in the bars interact with the rotating flux and produce torque. The operation of the motor during a start is similar to an induction motor. The LSPM has magnets in the rotor which pulls it into synchronism. The magnets cause oscillatory torque at all non-synchronous speed and also a net braking torque.

2.1.1. Braking torque in LSPM

The motor will start[1] if the asynchronous torque generated by the cage is more than the sum of the load torque and the braking torque from the magnet. As mentioned earlier, magnets in the motor cause braking torque because of the generating action. During transient operation, the rotating magnetic flux from magnets induces emf in the stator in as similar manner as in generator operation. As the speed of rotor is not synchronous the induced emf causes sub-harmonic currents in the

[1] In this thesis the start of a motor refers to its properties at standstill. After that begins the transient operation which ends when the motor goes into steady state through the synchronization process.

stator and produces a braking torque [3]. The magnets also produce other oscillatory torques given in [7]. Figure 2.1 shows asynchronous cage torque with magnets and without magnets over the speed range. It is clear that in the presence of magnets the asynchronous cage torque is reduced. Also it should be noticed that the maximum braking torque occurs at low speed. The slip corresponding to the maximum braking torque is given by equation 2.2 [5]. Hence the LSPM is a good choice for the applications where the load increases with increasing speed as in water pumps etc.

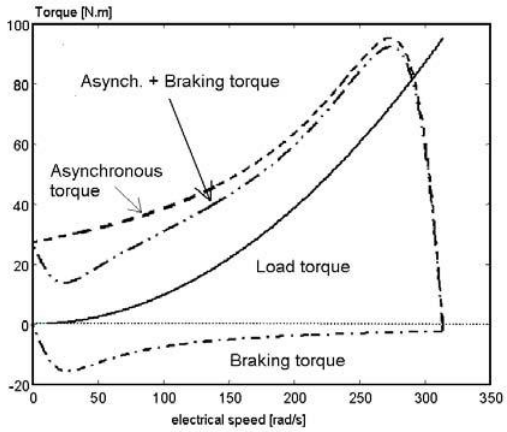

Figure 2.1.: Asynchronous cage torque with magnets and without magnets in LSPM [2]

Hence in the design of LSPM braking torque must be taken into consideration. The braking torque can be calculated analytically by equation 2.1 [5]. The derivation of the equation in detail can be found in [5]. The equation gives the variation of the braking torque with respect to slip.

$$T_b = \frac{3}{2}.\frac{p}{2}.\frac{1}{\omega_s(1-s)}\left[\frac{R_s^2 + x_{qs}^2(1-s)^2}{R_s^2 + x_{qs}x_{ds}(1-s)^2}\frac{R_s(1-s)^2}{R_s^2 + x_{qs}x_{ds}(1-s)^2}E_0^2\right] \tag{2.1}$$

$$s_{bm} = 1 - \frac{R_s}{\sqrt{2}}\frac{\sqrt{3(x_{qs}-x_{ds}) + \sqrt{9(x_{qs}-x_{ds})^2 + 4x_{qs}x_{ds}}}}{x_{qs}\sqrt{x_{ds}}} \tag{2.2}$$

In equation 2.1 and 2.2, T_b is the net braking torque, s_{bm} is slip for maximum braking torque, E_0 is the open circuit voltage at rated synchronous speed, ω_s is the synchronous angular speed, p is number of poles, s is slip , R_s is the stator resistance, x_{qs} and x_{ds} are the q and d axis reactances, respectively.

From equation 2.1, it is clear that the braking torque increases if E_0 is increased or if the q axis reactance increases. Therefore, to decrease braking torque either magnets volume or reluctance asymmetry needs to be reduced. Nevertheless, sufficient magnetic torque, reluctance torque or both are required to pull the motor into synchronization. Both the braking torque and synchronization torque are sum of reluctance and magnet torques. Therefore, if the reluctance in the motor can be increased the magnets volume can be reduced without affecting the starting and synchronization of the motor.

2.1.2. Effect of rotor position at start

When a motor is supplied with a voltage source it creates stator flux. This stator flux interacts with the flux from the permanent magnet in the rotor. The generated torque from the interaction of stator flux and magnetic flux depends on the angle between the flux vectors. The torque is given by equation 2.3 as,

$$T = k.|\overline{\psi_m}.|\overline{\psi_s}|.sin(\delta) \tag{2.3}$$

where, T is the torque, $\overline{\psi_m}$ is rotor magnet flux vector, $\overline{\psi_s}$ is stator flux vector and δ is the angle between two flux vectors.

From the equation it can be seen that torque depends on the angle δ if the magnitudes of the flux vectors are kept constant. Now if the angle δ is between 0 to π the torque generated will be positive and good for starting. If the angle is between π to 2π the torque will be negative and will deteriorate the starting performance. The flux vectors at optimal and worst positions of the flux vector are shown in figure 2.2.

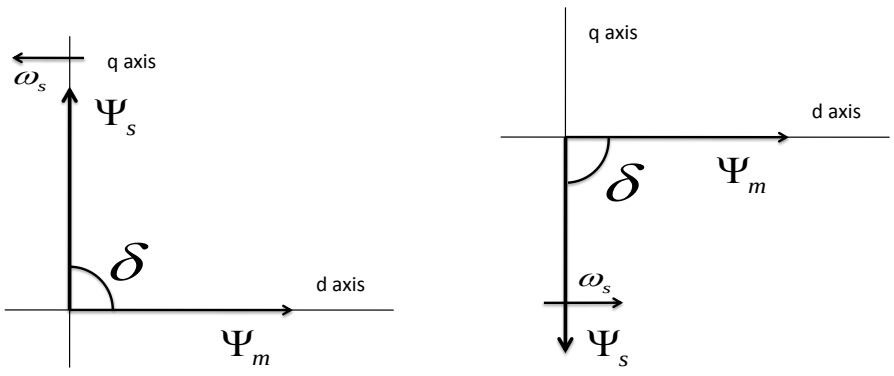

(a) Optimal start (b) Worst start

Figure 2.2.: Flux vectors position for optimal and worst condition for the start

Figure 2.2(a) shows the optimal case for start when angle δ is equal to $\pi/2$. The torque generated at this instant is maximum and positive. This torque improves the starting torque. The stator flux is rotating with synchronous speed but the rotor flux has zero speed and because of the inertia of the motor, rotor speed will change gradually. This will make angle δ to increase and the torque to decrease till the angle δ exceeds π. In practical the best start is when δ is 0 because of mechanical constraints. The mechanical system is designed to start with only asynchronous torque. In the optimal start the synchronous torque is very high which will result in a very high total starting torque (synchronous torque+asynchronous torque). This high starting torque is undesirable for the mechanical system attached to the motor.

Figure 2.2(b) shows the worst starting scenario. The rotor position is such that the stator flux is lagging the rotor flux by $\pi/2$. The torque at that instant is again maximum but negative. In this condition the starting torque will be reduced. The angle δ will reduce and the torque will become positive once the stator flux crosses the rotor flux vector. This could cause a very slow and oscillatory start.

The effect of reluctance torque in the starting of a motor is not considered here. The reluctance torque also depends on the position of the rotor. The LSPM has very low reluctance torque hence it will not affect the starting performance much. It would however, interesting to further study the dependency of starting torque in the motor to both the magnetic as well as reluctance torque.

2.2. Steady State operation

In steady state the LSPM works like a synchronous motor. Therefore, it exhibits performance of a synchronous motor. LSPM goes through a important phenomenon of synchronization before entering in steady state. The capability of synchronization of the motor depends on many factors described next in this chapter.

2.2.1. Synchronization of LSPM

Synchronization is the process in which the motor goes from transient to steady state operation. The total asynchronous cage torque accelerates the motor from standstill to speed close to the synchronous speed. Once the mechanical speed reaches close to synchronous speed the motor should have enough synchronous torque to pull the motor in synchronization. The synchronizing torque of the motor at any rotor speed is given by equation 2.4,

$$T_s(\delta) = \frac{k}{\omega_m}\left[\frac{EU}{x_{ds}}sin(\delta) - \frac{U^2}{2}\left[\frac{1}{x_{ds}} - \frac{1}{x_{qs}}\right]sin(2\delta)\right] \tag{2.4}$$

where T_s is the synchronous torque, k is a constant, ω_m is the mechanical speed, δ is the load angle and U is the supply voltage.

As long as motor is not synchronized, the load angle keeps on changing as stator flux vector and rotor flux vector will have a relative angular velocity. If the load angle is an integral multiple of 2π the net effect of synchronous torque on motor speed will be zero theoretically. At low speed, the relative speed between the stator flux and rotor flux is very high and the load angle changes very rapidly. Thus at low speed synchronous torque does not add to the net acceleration torque of the motor.

When the speed reaches near synchronous speed the relative speed between stator flux and rotor flux become small and hence the frequency of oscillation will also be small. Therefore, synchronous torque changes slowly. The acceleration generated by the synchronous torque changes the speed of the motor and pulls the motor in synchronization. The synchronous torque cycle for a successful synchronization based on the equation 2.4, is shown in figure 2.3 .

During synchronization the asynchronous torque also act. This torque helps in the synchronization as it accelerate the motor below synchronous speed and decelerate the motor above synchronous speed [5]. For simplification the effect of asynchronous torque in synchronization is not considered. The synchronization process including all the torque components is discussed in detail in [3],[8].

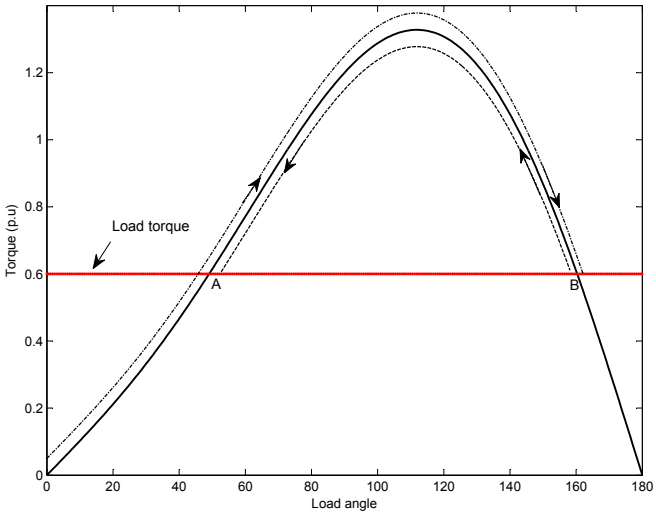

Figure 2.3.: Synchronous torque variation with load angle

The synchronization process starts when the synchronous torque become positive. Referring to figure 2.3 at point 0, the motor will have some positive slip at that instant and hence the motor will be accelerating. This will make the load angle δ to increase. With the increase in angle the synchronous torque will increase. At point A in figure 2.3 the synchronous torque becomes equals the load torque. At this point the motor will still accelerate because of the positive slip. Thus the synchronous torque will become higher than the load torque and accelerate the motor further. The motor synchronizes if it reaches the synchronous speed before point B i.e. slip equals to 0. It is advantageous to have low slip at the start of synchronization as lower slip ensure lower energy requirement to synchronize [8].

When the motor reaches synchronous speed before point B, the synchronous torque will be higher than the load torque which will take the speed of the motor above synchronous speed. But the load angle will start decreasing as the relative angle between rotor flux vector and stator flux vector will become negative. The motor will move to point A shown in the figure 2.3 which will become the steady state operating point. The synchronization process for the motor with high reluctance torque is also the same except for the difference in the periodicity of torque variation with load angle. It can be seen from the equation 2.4 that the flux alignment torque has a period double that of reluctance torque.

The various parameters that effects the synchronization process are as follows:

- **Total inertia and load torque :**The inertia and load torque are very critical for the successful synchronization. With an increase in inertia the motor's capability to synchronize decreases and vice versa. Figure 2.4 [3] shows the critical inertia of the motor that can be synchronized at a function of load. From the figure it is clear that with change in load the critical inertia changes drastically and synchronization is very sensitive to both parameters.

- **Supply voltage :** From equation 2.4 it can be seen that the synchronous torque depends on the supply voltage. The flux alignment torque depends on the supply voltage linearly and the reluctance torque of the motor varies with square of voltage. The motor with high flux alignment torque is less sensitive to supply voltage than the motor with high reluctance torque. Therefore, the synchronization of the motor is sensitive to supply voltage. The transient state also depends on the supply voltage. Higher the supply voltage higher will be the asynchronous torque and hence greater acceleration. Therefore, synchronization will start at lower slip. The lower slip helps the synchronization indirectly as energy required for synchronization will be less [8].

- **Magnet volume used :** The addition of magnet increases the synchronous torque by increasing air gap flux density. The increase in synchronizing torque improves the synchronization process. But as mentioned earlier in section 2.1.1,the magnets also cause braking torque. Increase in magnet volume will increase the braking torque and eventually reduce the accelerating torque.

Hence magnet volume has to be optimized to different load torque [8] and also to keep balance between the transient and steady state performance.

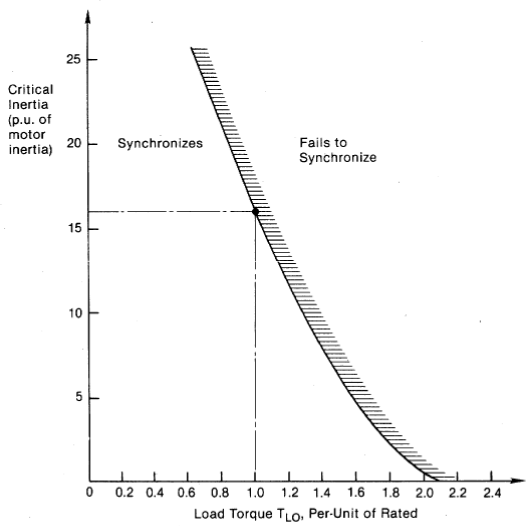

Figure 2.4.: Synchronization of PM motor with Inertia and torque [3]

- **High saliency ratio :** The motor with high reluctance torque has to be designed with high saliency. Like the flux alignment torque, increasing the reluctance torque increases synchronizing torque which gives better synchronization. High reluctance torque means high steady state torque which improves efficiency. Increasing saliency however, increases the reluctance torque upto a limit and after that torque decreases because of cross magnetization [9],[10]. Saliency also improves the power factor of the motor. Figure 2.5 [4] shows the variation of power factor of a purely reluctance motor(no magnets)with saliency. The relation between maximum power factor and saliency of a purely reluctance motor is given by 2.5 [11]. From the equation it is clear that as the saliency will increase the power factor will improve. The change in power factor at low saliency is high but as the saliency is increased the power factor change is reduced. Therefore, even with very high saliency the power factor of pure reluctance motor cannot match the power factor of PM motors. The power factor of pure reluctance motor can be increased by adding some magnets to attain the desired power factor.

$$PF = \left[\frac{L_d}{L_q} - 1\right] / \left[\frac{L_d}{L_q} + 1\right] \tag{2.5}$$

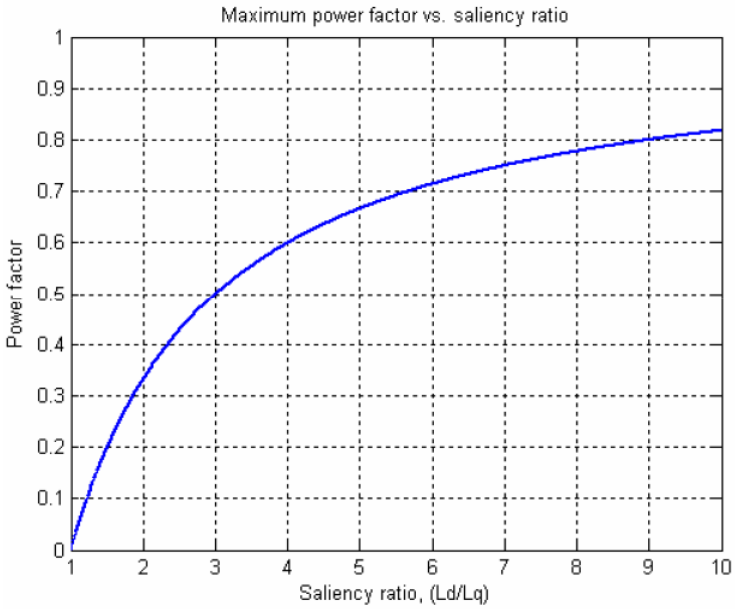

Figure 2.5.: Variation of maximum power factor with saliency for a purely reluctance motor(no magnets)[4]

2.2.2. Synchronous Torque

The steady state performance of the LSPM depend on the synchronous torque. The torque is the sum of both the flux alignment torque and the reluctance torque. Hence synchronous torque can be varied by varying either torque. The synchronous torque for LSPM is given by equation 2.6 [5]. The synchronizing torque given in by equation 2.4 equals the synchronous torque at synchronous speed.

$$T_s(\delta) = \frac{3p}{2\omega_s}\left[\frac{EU}{x_{ds}}sin(\delta) + \frac{U^2}{2}\left[\frac{1}{x_{qs}} - \frac{1}{x_{ds}}\right]sin(2\delta)\right] \tag{2.6}$$

As mentioned earlier the synchronous torque is the sum of flux alignment torque and reluctance torque. The interaction between the stator flux and rotor flux cause flux alignment torque. The variation in reluctance along the rotor seen by the stator flux causes the reluctance torque. The reluctance torque forces the rotor to align itself along the lowest reluctance path as seen by the stator flux. Therefore, without saliency in the rotor there will no reluctance torque.

Figure 2.6 shows the variation of synchronous torque, reluctance torque and flux alignment torque with load angle. The reluctance torque has period double of flux alignment torque. It can also be seen that the maximum of synchronous torque

occurs at load angle around 110 degree for $x_d < x_q$ whereas for $x_d > x_q$ the maximum occurs at around 70 degree.

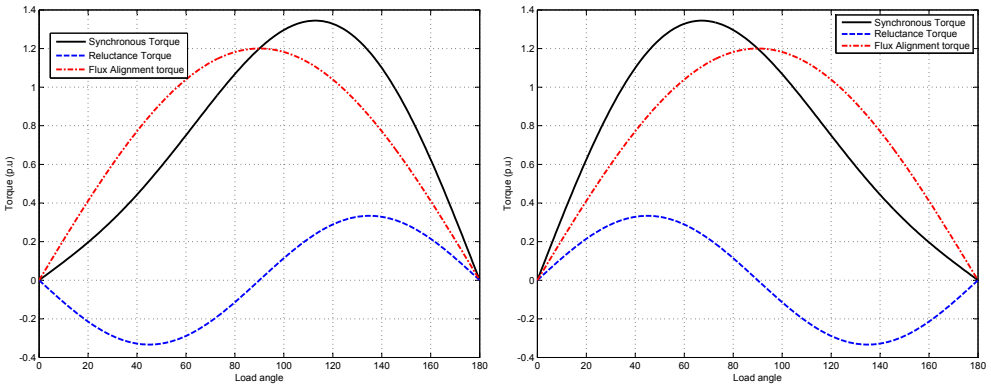

(a) Different torque with $x_d < x_q$ (b) Different torque with $x_d > x_q$

Figure 2.6.: Variation of synchronous torque,reluctance torque and flux alignment torque with load angle

The LSPM motor has $x_d < x_q$ because the flux in the d direction has to cross the air gap as well as the magnet slots whereas in the q direction it only has to cross the air gap. Therefore, the reluctance in the q direction will be lower than the reluctance in the d direction. Hence the reactance in the d direction will be lower than in the q direction. The variation of torque with load angle in LSPM for this case is shown in figure 2.6(a). The flattening of the torque at lower load angle is due to the reluctance torque. If the saliency of the motor is increased keeping the magnet volume constant the flattening increases as shown in figure 2.7.

As the saliency is increased the maximum torque increases and also the load angle for maximum torque is changes slightly as shown in figure 2.7. Therefore, to obtain same maximum torque the reluctance torque can be increased and correspondingly the volume of magnet can be reduced. However, as mentioned earlier after a certain value of saliency the reluctance torque does not change much. Hence, to match the performance of a LSPM with a purely reluctance motor is very difficult.

Synchronous torque for different magnet volume and reluctance torque is shown in figure 2.8. In figure 2.8(a) synchronous torque is calculated with saliency equal to 2 and back EMF(E_o) equal to 0.9 p.u while in figure 2.8(b) synchronous torque is calculated with saliency equal to 6 and back EMF(E_o) equal to 0.35 p.u. In both the cases the maximum synchronous torque is the same but the back emf is reduced to 0.35 p.u from 0.9 p.u. Therefore, by increasing reluctance torque

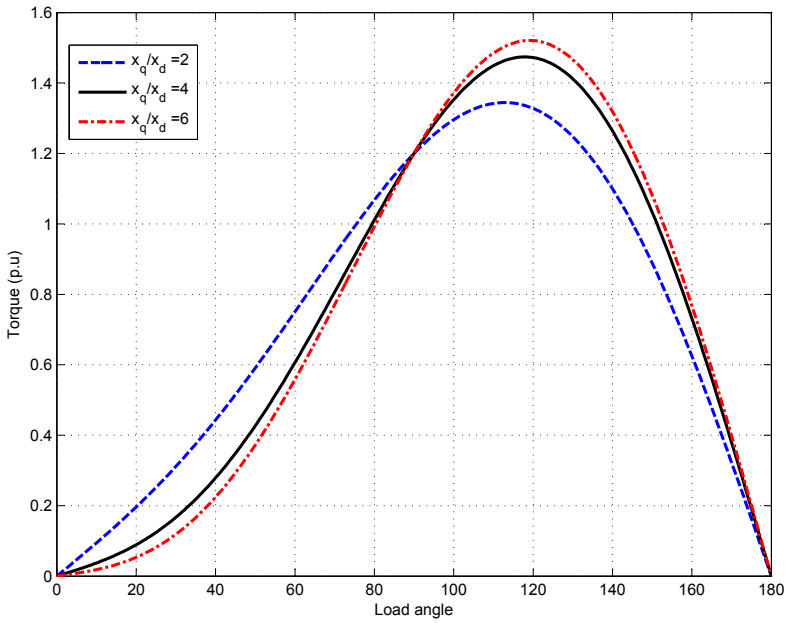

Figure 2.7.: Effect of saliency on synchronous torque

the volume of magnet required can be reduced to achieve a motor with the same performance.

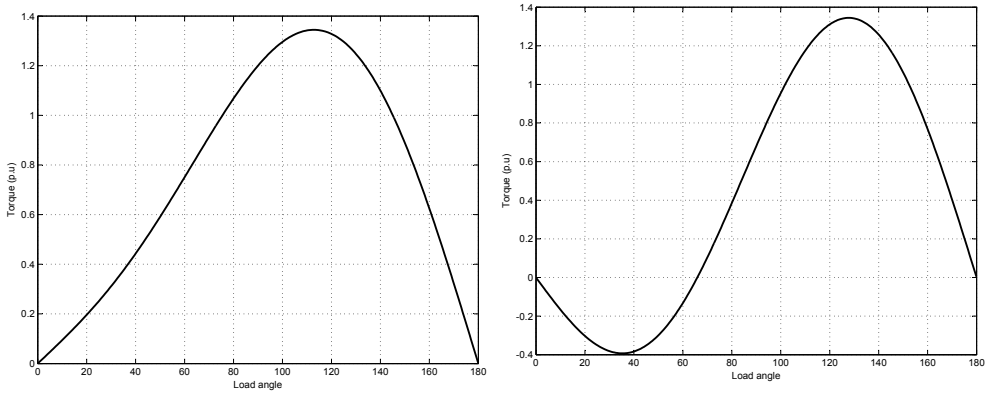

(a) Torque with $x_q/x_d = 2, E_o = 0.9$ (b) Torque with $x_q/x_d = 6, E_o = 0.35$

Figure 2.8.: Synchronous torque for different magnet volume and saliency

3 Chapter 3
Use of Flux Barrier and Two different grade Magnets

In this chapter, the effect of using flux barrier on the leakage of magnetic flux is presented. Also the effect of using two different grades of magnets on air gap flux density is calculated and discussed.

The calculation was done using FEM model of a 4 pole LSPM. The cross section of the motor is shown in figure 3.1. The construction of motor is similar to a PM motor except the squirrel cage. The function of cage is to make motor self-start like an induction motor. The magnets are placed in U shape which increases the effective coverage area of magnet and thus improves the air gap flux density. The magnets used in the motor are NdFeB(Br is $1.14T$ and permeability (μ_r)is 1.05 at 20^oC). All magnets in the motor are of same size and shape.

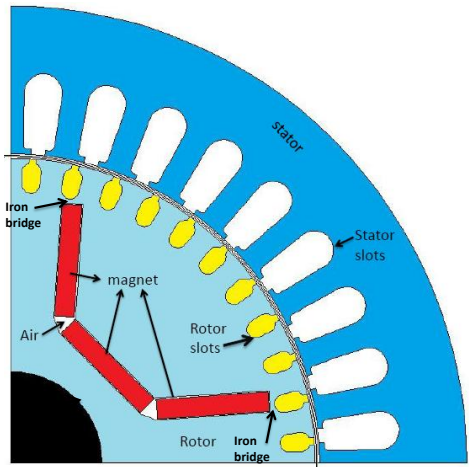

Figure 3.1.: Cross section of LSPM

In figure 3.1, it can be seen that some air is present between two adjacent magnets.

The air between the magnets acts as a flux barrier and reduces the magnetic flux leakage. However, the iron bridges present between the magnets and the rotor slots cause leakage of flux.

3.1. Flux Barrier

As mentioned above, the iron bridge causes leakage of magnetic flux. The magnetic flux flows through minimum reluctance path. The iron bridge provides minimum reluctance path until it gets saturated. Therefore, maximum leakage of flux takes place because of iron bridges in the rotor. The saturation of the iron bridge depends on its thickness. The bridge reaches saturation at lower flux density if thickness of the bridge is less. Thus, the magnitude of the leakage flux is very sensitive to the thickness of the iron bridge. The thickness of iron bridge in LSPM is 1mm. The thickness cannot be reduced further because of manufacturing constraints. The magnetic flux distribution in LSPM is shown in figure 3.2.

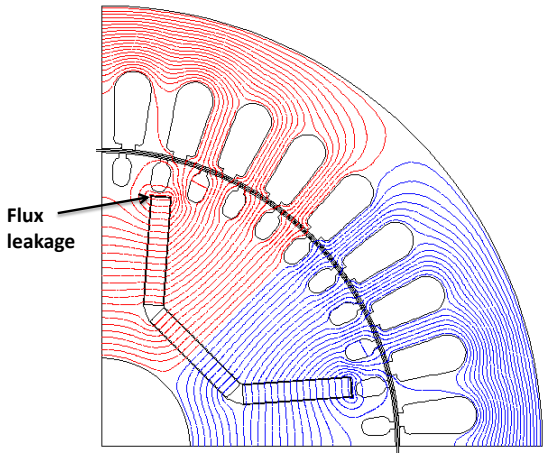

Figure 3.2.: Magnetic flux lines distribution in LSPM.

As seen in figure 3.2, the magnetic flux leakage through the iron bridges is more compared to the air between the adjacent magnets. The air between the magnets provides flux path with higher reluctance compared to iron bridges. Therefore, introducing flux barriers will reduce flux leakage and moreover, may save some magnet used in the motor.

To understand the effect of flux barrier, the magneto static calculation was done using software Flux 2D (by Cedrat). The motor geometry with flux barriers, as shown in figure 3.3, was simulated. The resulting fundamental component of air-gap flux density was compared with the flux density in LSPM without barriers. The

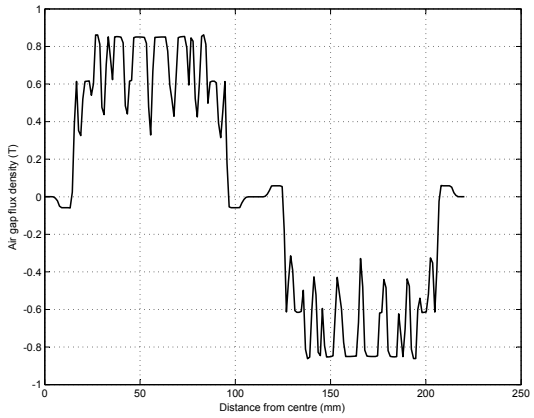

Figure 3.3.: Air gap flux density in LSPM

air-gap flux density of the LSPM without flux barriers is shown in figure 3.3. The fundamental component of the flux density is 0.778 T at 20^oC. The trapezoidal shaped barrier was used in simulation. The flux distribution with the barrier is shown in figure 3.4. Comparing figure 3.2 and figure 3.4, it is clear that flux barrier reduced the leakage of magnetic flux through iron bridge is reduced.

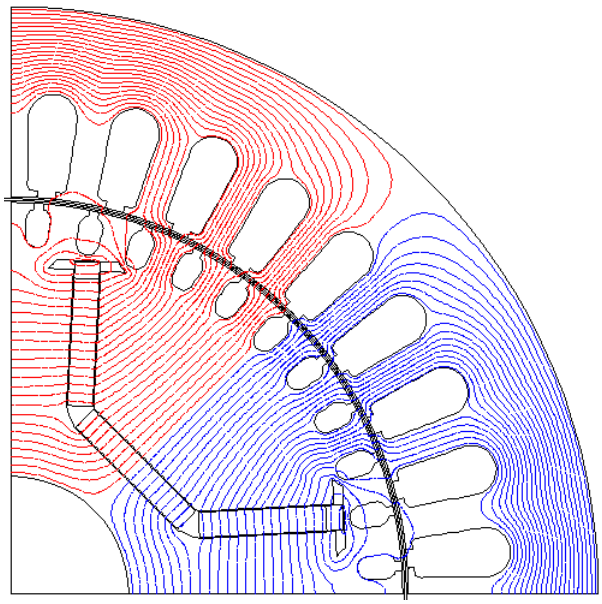

Figure 3.4.: Flux lines distribution with trapezoidal flux barrier

The dimensional parameters of the flux barrier are shown in figure 3.5. The air gap flux

density at different barrier length and barrier width was calculated. In figure 3.6(a), the change in fundamental component of the flux density at different barrier length (A_L) is shown, while other parameters kept fixed. Similarly figure 3.6(b) shows the effect of change in barrier width (A_w) on flux density[1].

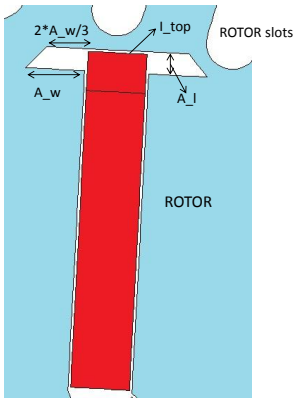

Figure 3.5.: Trapezoidal flux barrier geometry

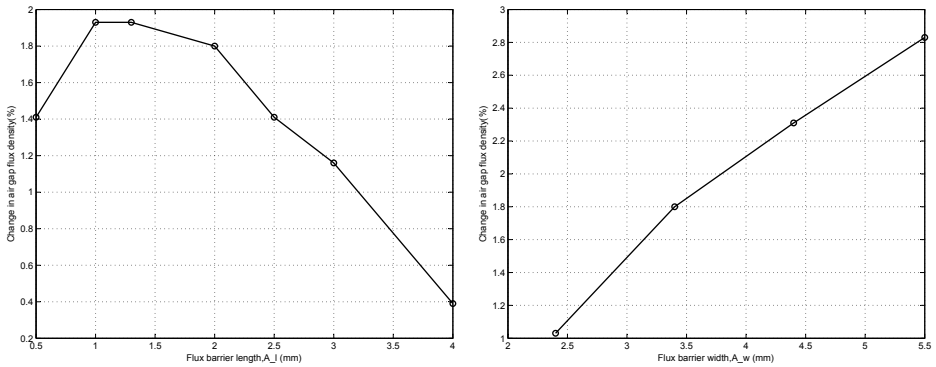

(a) Flux density change vs Barrier length A_w=3.4mm, I_top=0.2mm

(b) Flux density change vs Barrier width A_l=2mm, I_top=0.2mm

Figure 3.6.: Effect of trapezoidal flux barrier on air gap flux density

It can be seen from figure 3.6 that the flux barrier improved the air gap flux density. It can also be observed that initial increase in the barrier length caused increase in flux density. When the barrier length was increased further it started obstructing the

[1]The change in flux density is calculated with respect to the air-gap flux density (0.778 T), the flux density in LSPM without barriers.

useful magnetic flux, and thus caused reduction in air gap flux density. The air gap flux density increased with increase in barrier width as shown in figure 3.6 (b). The increase in barrier width decreases the bridge thickness which causes reduction in leakage. However, the bridge thickness should not be smaller than 1mm and hence limits the barrier width.

The air-layer (I_top) on the top of magnets also influences the air-gap flux density and thus critical in designing the flux barrier. The I_top cannot be reduced less than 0.2 mm due to manufacturing limitations. The I_top was increased and the corresponding length of magnets was decreased so that the thickness of iron bridge kept fixed at 1 mm. The air-gap flux density at different values of I_top was calculated and given in Table 3.1. The length and breadth of the barrier were kept fixed while calculating the flux density.

I_top (mm)	**Magnet length** (mm)	**Flux density** (T)
0.2	25.8	0.79
0.4	25.6	0.788
1	25	0.773
1.2	24.8	0.778
1.4	24.6	0.775
2.4	23.6	0.76

Table 3.1.: Flux density variation with length of air at top of magnet(I_top) with A_l=1.5mm,A_w=2.5

From the table 3.1, it can be seen that when I_top was increased the flux density decreased because of decrease in the magnet length. It can also be observed from the table that air-gap flux density was 0.778 T (flux density in LSPM without barriers) with 2.5% less magnet volume when the barriers of mentioned dimensions were used.

3.2. Use of two different grades of magnets

Use of two different grades of magnet can be useful in reducing the cost of the magnet used in the motor. The selection of magnet material in the motor mainly depends on the operating condition as well as the application of motor. The operating condition in the motor varies from one part to another. Hence, different magnet materials can be used at different parts. The effects of using Ferrite or SmCo magnets along with NdFeB magnets were studied and results are presented in this section. The different grades of magnets were arranged in the motor as shown in figure 3.7. The total volume of the magnets were kept fixed. The material used for magnet 1(M1) and magnet 5(M5) were same and also their dimensions were equal. The material

used for magnet 2(M2) and magnet 4(M4) were same and also their dimensions were equal. The dimensions and material of magnet 3(M3) were kept same as in LSPM.

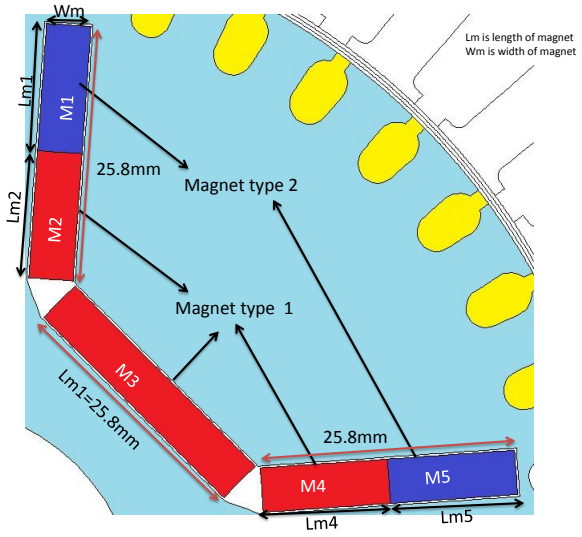

Figure 3.7.: Magnet arrangement of two different grades

3.2.1. Using NdFeB and SmCo magnets

The remanent flux density (Br) of SmCo and NdFeB magnets are in the range of 1-1.1 T at temperature 20^oC. However, SmCo magnets have lower temperature coefficient than NdFeB magnets. Hence, SmCo magnets better for high temperature applications. Another advantage of SmCo magnets is better resistivity to corrosion than NdFeB magnets. However, the price of SmCo is higher than NdFeB at present. Above mentioned advantages and disadvantages make it interesting to study the effect of SmCo magnets along with NdFeB magnets in the motor operation. Some of NdFeB (Br is $1.14T$ and permeability is 1.05 at 20^oC) magnets were replaced with SmCo (Br is $1.1T$ and permeability is 1.06 at 20^oC) magnets. The length of different magnets and the calculated air-gap flux density are given in table 3.2.

M1(SmCO) Lm1(mm)	**M2(NdFeB)** Lm2(mm)	**M3(NdFeB)** Lm3(mm)	**SmCo** (%)	**Flux density** (T)
1	24.8	25.8	2.6	0.777
2	23.8	25.8	5.2	0.777
12.9	12.9	25.8	33.3	0.77
23.8	2	25.8	61.5	0.763

Table 3.2.: Air gap flux density using SmCo and NdFeB magnets

It can be seen from table 3.2 that the fundamental component of air-gap flux density is not varying much by replacing NdFeB with SmCo magnets. It was expected as the Br and μ_r of SmCo magnets are similar to NdFeB magnets. At high temperature, around 140^oC, the Br of SmCo and NdFeB have significant difference. However, the operating temperature of the motor was not taken in account during simulation. Hence, the effect of temperature is not seen in the results calculated.

The magnet 3(M3) was replaced with SmCo while other magnets were NdFeB. The calculated fundamental flux density was 0.77 T. Now, when all magnets were SmCo magnets the fundamental air gap flux density was 0.737 T. The difference in flux density is because of the slight difference in remanent flux of NdFeB ($B_r = 1.14$ at 20^oC) and SmCO ($B_r = 1.1$ at 20^oC).

3.2.2. Using NdFeB and Ferrite magnets

The magnets arrangement was same as shown in figure 3.7. Magnets M1 and M5 were replaced with ferrite magnet (Br is $0.41T$ and permeability is 1.36 at 20^oC). The rest of the magnets were kept NdFeB. The air-gap flux density was calculated at different ferrite magnet volume is given in table 3.3. The ferrite has very low remanent flux at 20^oC than NdFeB magnet. Hence, the air gap flux density decreased rapidly with increase in ferrite volume.

M1(Ferrite) Lm1(mm)	**M2(NdFeB)** Lm2(mm)	**M3(NdFeB)** Lm3(mm)	**Ferrite** (%)	**Flux density** (T)
1	24.8	25.8	2.6	0.764
2	23.8	25.8	5.2	0.753
3	22.8	25.8	7.8	0.74
12.9	12.9	25.8	33.3	0.599
25.8	0	25.8	66.7	0.411

Table 3.3.: Air gap flux density using Ferrite and NdFeB magnets

The price of ferrite magnet is much lower than NdFeB magnets. Thus, even if the double amount of ferrite magnet is used, the total cost of magnet in the motor will be less. This makes ferrite magnet an attractive choice. Therefore, the motor was simulated with more magnet volume than in LSPM. Figure 3.8 shows the magnets slot shape for magnet M1 and M5. The magnet slots for M2, M3 and M4 were kept same as shown in figure 3.7

The air-gap flux density was calculated at different ferrite magnet length while the width (F_w) of the magnet kept fixed and is given in table 3.5. When the length of ferrite magnet was changed the corresponding length of NdFeB magnet (Lm2) was also changed to keep the thickness of iron bridge 1 mm. Also the flux density was

calculated at different ferrite magnet width while magnet length (F_l) of the magnet was kept fixed and is given in table 3.4.

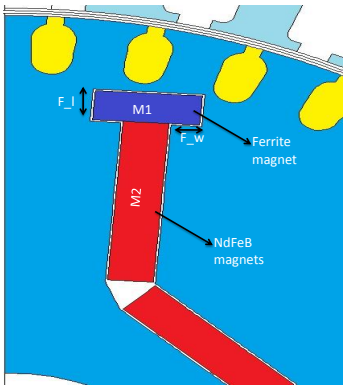

Figure 3.8.: Magnet arrangement with Ferrite and NdFeB magnets

F_w (mm)	**Ferrite Volume** (%)	**Flux density** (T)	**Flux density change** (%)
0.1	8.07	0.748	-3.86
0.3	8.70	0.751	-3.47
0.5	9.31	0.753	-3.21
0.7	9.92	0.756	-2.83
1	10.82	0.759	-2.44
1.5	12.29	0.764	-1.80
2	13.70	0.769	-1.16
2.5	15.07	0.774	-0.51
3	16.39	0.778	0.00

Table 3.4.: Air gap flux density at different volume of ferrite magnet(keeping magnet length fixed F_l =3mm, NdFeB magnets length(Lm2,Lm4) is 22.8mm and Lm3=25.8mm)

F_l (mm)	**Ferrite Volume** (%)	**Flux density** (T)	**Flux density change** (%)
1	3.16	0.792	1.80
2	6.13	0.785	0.90
3	8.93	0.778	0.00
4	11.56	0.77	-1.03

Table 3.5.: Air gap flux density at different volume of ferrite magnet(keeping magnet width fixed F_w=3mm)

In table 3.4, the change in flux density is not large with the change in magnet width.

This is because the magnetic flux depends on the length of magnet perpendicular to the lines of flux. However, the small change in flux density is due to reduction in the thickness of iron bridge (iron between magnet and adjacent rotor slot) when magnet width was increased. Therefore, the flux density increased mainly because of reduced flux leakage.

From table 3.5, it can be seen that the flux density decreased with the increase in ferrite length. The flux density decreased because the NdFeB magnets (Lm2, Lm4) length reduced with the increase in ferrite magnets length. It can also be seen from the table that the change in flux density is 0 with 3 mm (length) ferrite magnet. Therefore, 7% of the NdFeB magnets can be saved, without changing the air gap flux density, if ferrite magnet is used.

Now, flux density was calculated by introducing flux barrier along with different magnetic materials (NdFeB and Ferrite) in magnet slots. The geometries of magnet slots and the barrier used are shown in figure 3.7 and figure 3.5 respectively. The calculated flux density is given in table 3.6. Comparing table 3.4, table 3.5 and table 3.6 it can be seen that the width of the magnet does not influence the air-gap flux density significantly. The flux density with 3 mm (length) ferrite magnet produced almost same change in flux density as with more ferrite magnet.

Ferrite length F_l(mm)	**NdFeB Length** Lm2(mm)	**Flux density** (T)	**Flux density change**(%)
1	24.8	0.791	1.67
2	23.8	0.782	0.51
3	22.8	0.771	- 0.9

Table 3.6.: Air gap flux density at different volume of ferrite and NdFeB magnets with barrier dimensions are A_w=4.5mm,A_l=1.7mm , I_top = 0.2mm

3.3. Summary

The introduction of flux barrier in the motor reduced the flux leakage through iron bridge. However, the reduction in magnet volume using flux barrier is not large. As mentioned earlier, the thickness of iron bridge significantly influence the magnetic flux leakage. Thin iron bridge can cause two problems. Firstly, the mechanical strength of the rotor will reduce. Secondly, it could damage the manufacturing tool. Therefore, the thickness of the iron bridge cannot be reduced after a limit.

Two different grades of magnets can be used to reduce magnet volume without affecting the performance of the motor. The selection of magnets depends on the operating condition of the motor. Also using two grades of magnets can reduce total cost of magnet for example, replacing some NdFeB magnets with Ferrite magnets. As it is presented in section 3.2.1, using SmCo in place of NdFeB magnets

produced almost same air gap density and also the price of SmCo and NdFeB is similar. Hence, replacing NdFeB with SmCo with respect to cost of magnet is not lucrative. Ferrite magnets are cheaper than NdFeB magnets however, as presented in section 3.2.2, reduction in NdFeB magnet volume is not large. In PM motors, the performance of magnet changes with the operating temperature of the motor. The operating temperature of motor in water pump application is generally in the range of $20^oC - 80^oC$ as there is no rotor loss and also the water cools the motor. The magnetic properties of SmCo and NdFeB do not vary much in this temperature range. Hence, the temperature does not play critical role in magnet performance for water pump motors. In line start motors the magnet selection depends mainly on its intrinsic coercivity (H_c). The coercivity of the magnet should be large enough to resist demagnetization, during the starting of the motor, because of high stator field.

Also using two magnets of different permeability changes the magnetic circuit of the motor. The change in magnetic circuit can significantly change the machine performance in steady state operation. Therefore, only magneto-static calculation will not give correct estimate of motor performance. The flux produced by magnets depends on the length of magnet surface perpendicular to the flux lines. Nevertheless, certain thickness of the magnet is required to ensure that the magnet does not demagnetize permanently. Moreover, thin magnets are very hard to manufacture. Also, while selecting the magnet material the position of the magnet in the rotor should be kept in consideration. The magnet near the air-gap is more prone to demagnetization than the magnet away from the air-gap. Therefore, the magnet placed near to the air-gap should have high demagnetization resistivity than the magnets placed away from the air-gap. Thus, to estimate the volume of magnet required and it's effect on the performance of the motor, transient study must be done. However, as reduction in magnet volume using barrier or different grades of magnets is not significant, further study was not done.

Chapter 4

4 LSPM with high saliency

The total synchronous torque in LSPM is the sum of the flux alignment torque and the reluctance torque, as described in chapter 2. The performance of the motor depends on the total synchronous torque. However, the behaviour of the motor depends on the torque that dominate. For example, if flux alignment torque dominates the motor will behave like a permanent magnet synchronous motor, whereas if reluctance torque dominates the motor will behave like a synchronous reluctance motor.

As discussed in section 2.2.2, if reluctance torque in the motor is increased then the amount of magnet required can be reduced, to produce the same torque. In principle, the LSPM with high saliency works as a magnet assisted synchronous reluctance motor in steady state. In this chapter, the basic working of the synchronous reluctance motor is presented. The magneto-static as well as transient model of motor was simulated and the results are discussed. Based on the parametric study, a design of LSPM with high saliency is proposed and compared with an induction motor of same rating.

4.1. Basic working of synchronous reluctance motor

In synchronous reluctance motor (SynRM), the reluctance torque develops due to non-uniform magnetic path seen by stator field i.e. non-uniform reluctance. The non-uniform reluctance causes distortion in the field and produces torque such that the rotor gets aligned to the field. As the stator field is rotating, it causes continuous distortion in field and consequently produces continuous torque. The torque development depends on the degree of distortion in the field. Like flux alignment torque in PM motors, the average reluctance torque is zero at all speeds other than the synchronous speed.

The torque developed in a purely reluctance motor can be derived from the equation 2.6 by putting flux alignment torque equal to 0 i.e. motor with no magnets. The derived equation of the reluctance torque is given in equation 4.1. It can be deduced

from the equation, that the developed reluctance torque in the motor depends on two factors. Firstly, the supply voltage and secondly, the difference of the reactances in two axes. For any given supply voltage the maximum reluctance torque is produced by maximizing the saliency i.e. maximizing the difference of reactances in two axes. In equation 4.1, T_r is the reluctance torque at any load angle (δ).

$$T_r(\delta) = \frac{3p}{2\omega_s}\left[\frac{U^2}{2}\left[\frac{1}{x_{qs}} - \frac{1}{x_{ds}}\right] sin(2\delta)\right] \tag{4.1}$$

The saliency of the rotor can be created by introducing air in only one axis as shown in figure 4.1. Unlike PM motors, the dq axis in the reluctance motor is interchanged, shown in the figure. The flux lines distribution in the motor is shown in figure 4.2. The figure shows the flux lines distribution when stator field is aligned with q axis and with d axis. When stator field gets aligned to q axis, the flux lines has to cross the flux barrier (air) and the air-gap which increases the q axis reluctance. On the other hand, when the stator field is aligned to d axis the flux lines cross only the air-gap between the rotor and the stator. Therefore, the d axis reluctance is lower as compared to q axis reluctance, thereby produce torque. It can also be observed from the figure 4.2 iron ribs cause flux leakage when the stator field is aligned to q axis. The flux leakage increases the q axis reactance and thus decreases the difference of d and q axis reactances. Therefore, lower the iron rib thickness higher will be the produced reluctance torque.

One of the main drawback of reluctance motors is poor power factor compared to PM motors. Unlike PM motors, the reluctance motor draws magnetizing current from the main supply which lowers the power factor. However, the poor power factor of the reluctance motor can be improved by putting magnets in the flux barrier slots.

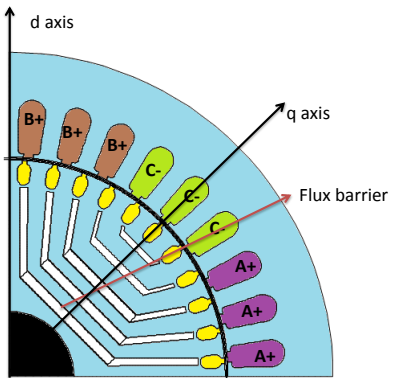

Figure 4.1.: Rotor geometry with barriers showing dq axis of the motor

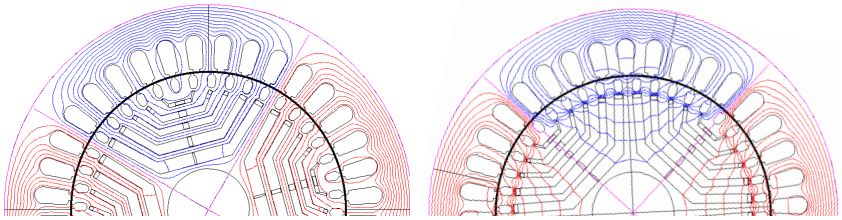

(a) Stator field aligned with d axis (b) Stator field aligned with q axis

Figure 4.2.: Flux lines distribution due to stator excitation only

4.2. Parametric Study

The performance of the motor depends on many factors like supply voltage, number of barriers etc. The number of poles in the motor is the also an important parameter which influences the performance of the motor. In this thesis however, the number of poles is kept fixed to 4. The different parameters and their effects are discussed in this section. Also the effect of magnet addition on the motor's performance is discussed.

4.2.1. Number of barriers

As discussed in section 4.1, the flux barriers create saliency in the rotor. The number of flux barrier in reluctance motor can be related to the rotor slots of an induction motor. For example, if a rotor has 11 slots per pole, then rotor slots 1,11 will make 1 barrier, slots 2,10 will make 2nd barrier and so on [12]. It is also important to note that the average reluctance torque depends on the total length of air introduced in the q direction. The air redistribution in flux barriers helps in smoothening of the developed torque [13]. Figure 4.3 shows rotor designs with three different number of barriers. The total length of air introduced in the q direction by barriers were kept equal. In other words, total widths of all barriers were kept equal in all designs.

The magneto-static model of the geometries, shown in figure 4.3, were simulated in FLUX 2D with equal current density. The maximum torque produced by the motor with 3, 4 and 5 barriers were calculated and is given in table 4.1. It can be seen from the table that the rotor geometry 2 has maximum saliency and thus produced maximum torque. The saliency of geometry 1 is slightly lower than geometry 2 due to increase in the q-axis flux density. In geometry 3, the iron between the barrier is thin because of high number of barriers and thus iron got saturated easily. The saturation of iron reduced the d-axis flux density and hence reduced the saliency.

Moreover, the q axis flux has also increased which further reduced the saliency and consequently geometry 3 produced lowest torque.

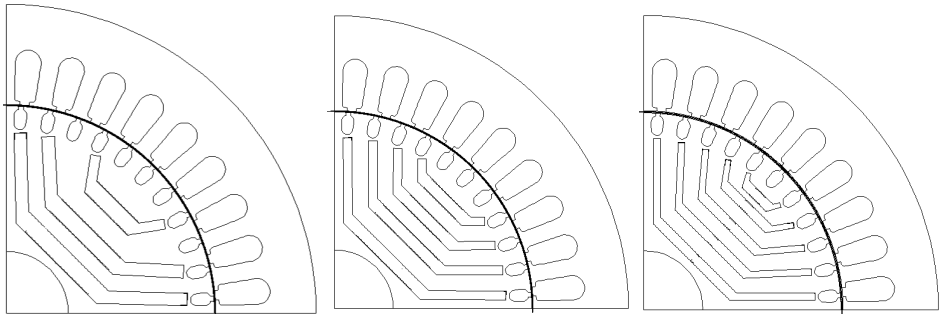

(a) geometry 1(3 barrier) (b) geometry 2(4 barrier) (c) geometry 3(5 barrier)

Figure 4.3.: Rotor geometry with different number of barriers with equal total width of barrier

	Torque (N.m)	q-axis flux density (T)	d-axis flux density(T)	L_d/L_q
Geometry 1	51.92	0.26	0.9	3.46
Geometry 2	55.4	0.234	0.91	3.89
Geometry 3	44	0.254	0.88	3.47

Table 4.1.: Change in d and q axis flux with number of flux barriers

The effect of flux barriers on transient operation was also studied. Now, the barriers in different geometries were rearranged such that they get aligned with the rotor slots as shown in figure 4.4. Figure 4.5 shows the transient behaviour of the geometries at rated load. With all three rotor geometries the motor can synchronize but they differ in the synchronization cycle as shown in figure 4.5(a). The first synchronization cycle for the geometries is between 0.1 s to 0.2 s. It can be seen that the slip at the start of synchronization is different for different geometry, which caused different synchronization cycle.

The developed synchronous torque also plays very important role in synchronization of the motor as explained in section 2.2.1. Figure 4.5(b) shows net total torque (magnetic torque - load torque) at different speeds. The torque response of all geometries is almost similar. However, to understand the role of synchronous torque in synchronization, it is important to consider the developed torque in the first synchronization cycle i.e. torque developed between 1200 rpm - 1400 rpm. From the figure it can be seen that geometry 1 has lower synchronous torque than geometry 2. On the other hand, figure 4.5(a) shows that geometry 1 has lower slip compared to the slip of geometry 3 at the start of synchronization process. Therefore, it is

easy for geometry 1 to synchronize despite the low synchronous torque [8]. From the speed response, as shown figure4.5(a) it can be seen that geometry 2 and geometry 3 has almost equal slip at the starting of synchronization cycle. However, geometry 2 synchronized earlier than geometry 3 because geometry 2 has higher net torque than geometry 3 as shown in figure 4.5(b). Therefore, the synchronization of motor depends on two factors firstly, slip at the start of synchronization cycle and secondly, the synchronous torque.

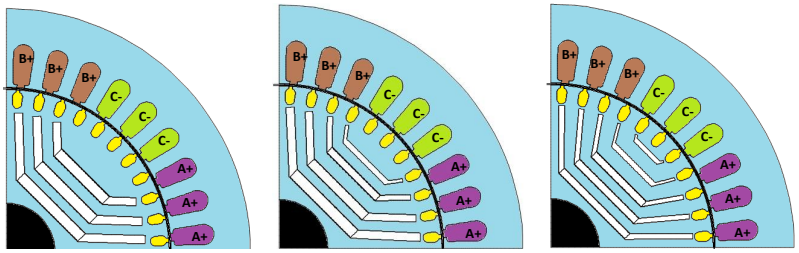

(a) geometry 1 (b) geometry 2 (c) geometry 3

Figure 4.4.: Rotor geometry with barriers rearranged

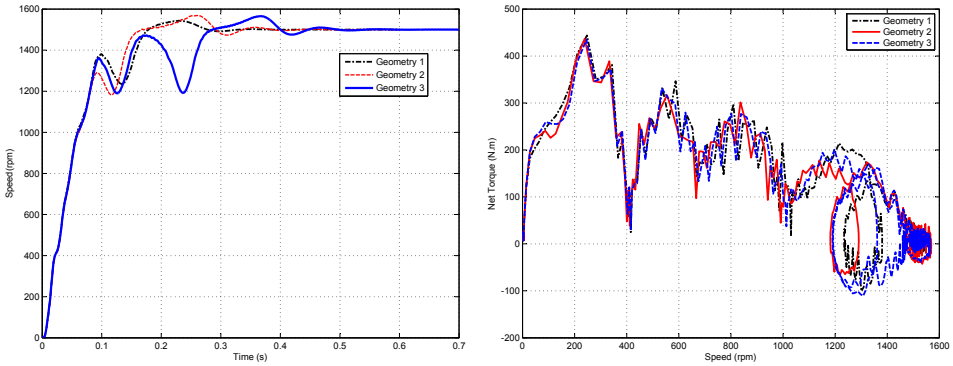

(a) Transient speed response (b) Net torque vs Speed

Figure 4.5.: Transient response of geometry 1,geometry 2,geometry 3 under load

When magnets are to be placed in barriers, it is important to consider the size of magnet while deciding number of barriers in the design. If number of barriers are more then the width of the barrier will be small. Consequently, width of the magnets will be small. Thin magnets are difficult to manufacture and are also prone to demagnetization which is not desired. On the other hand, if number of barriers number are fewer then width of the barrier will be large and so the width of the magnets. As presented in section 3.2.2, the magnetic flux contribution depends on the

magnet length. Therefore, the barrier should not be too wide nor it should be too thin. Hence, the magnet size puts a limitation on number of barriers.

4.2.2. Insulation ratio

Insulation ratio is defined as the ratio of air length to the total length of iron and air [4]. Mathematically, it can be written as given in equation 4.2. The different dimensions are shown in figure 4.6. The insulation ratio can be calculated for both q and d axes. As barriers are placed in alignment with rotor slots the effect of positioning of barriers with respect to d axis is not considered in the thesis. Thus, the insulation ratio in q direction is only calculated.

$$kq_{ins} = \frac{l_{air}}{l_{air} + l_{iron}} \tag{4.2}$$

In the above equation, kq_{ins} is insulation ratio in the q-direction, l_{air} is total length of air in q the direction, l_{iron} is total length of iron in q the direction .

Now, the rotor geometry 2 with 4 barriers as shown in figure 4.3 was simulated with different insulation ratios. The torque at different insulation ratios is given in table 4.2. It can be seen that as insulation ratio is increased the torque first increased and then decreased. When insulation ratio is increased the q-axis reluctance decreased as the air length in the q direction increased and thus q-axis reactance decreased. On the other hand, d-axis reactance is unchanged and consequently the developed reluctance torque increased. Increasing insulation ratio further (in this case more than 0.44) increased the q-axis reactance. Moreover, increase in the insulation ratio also decreased the d-axis reactance because of the saturation of iron. Hence, the difference between the reactances along the two axes decreased and consequently decreased the developed torque.

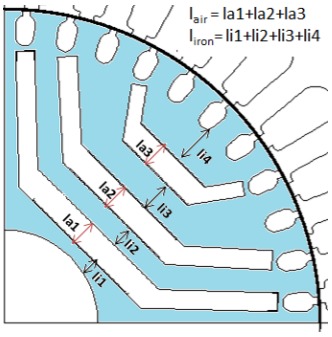

Figure 4.6.: Cross section of rotor showing different parameters

Insulation Ratio (kq_{ins})	Reluctance Torque (N.m)
0.25	51.99
0.29	52.80
0.35	54.75
0.4	54.76
0.44	55.28
0.49	54.68
0.54	53.21

Table 4.2.: Variation of reluctance torque with insulation ratio(kq_{ins})

The magnetic flux increases the saturation of iron and thus increases the reluctance in the d direction. Therefore, insulation ratio corresponding to maximum developed torque of the motor may vary with volume and material of the magnet used [13].

4.2.3. Effect of air gap length

Air-gap length influences both the d and q axes reluctances. Therefore, it is very important parameter influencing the performance of the motor, specially the reluctance motor. To study the effects of air-gap length, transient model of geometry 2 (see figure 4.4) was simulated with different air-gap lengths at rated load. The calculated efficiency[1] and power factor is given in table 4.3. The reduction in air-gap length reduced the line current and thus the efficiency and power factor improved. The d-axis reluctance changes significantly with the change in the air-gap length because the flux in the d direction only crosses the air-gap as shown in figure 4.2. One the other hand, the total air length in the q direction is sum of widths of flux barriers and the air-gap length. The air-gap length is a small part of total air length in the q direction. Therefore, small change in the air-gap length does not produce significant change in the q-axis reluctance. Thus, decreasing air-gap length increases the d-axis reactance, whereas q-axis reactance does not change. Hence, increases the difference of reactances and consequently increases the reluctance torque. The increase in reluctance torque reduces the current required to deliver the load torque and improves the efficiency. Moreover, decreasing air-gap length also improved the power factor. As mentioned above, d-axis reactance increases more than q-axis reactance when air-gap length is reduced and thus increases the saliency ratio L_d/L_q. The power factor of motor depends on the ratio L_d/L_q as given in section 2.2.1, more details are given in [4],[12],[11].

Air gap length (mm)	Line Current (A)	Copper loss (W)	Iron loss (W)	Efficiency (%)	Power Factor $cos(\phi)$
1	28.8	1321	134	89.6	0.70
0.75	26.6	1128	136.4	90.00	0.74
0.5	25	995	138.8	91.68	0.79

Table 4.3.: Effect of air gap length on performance of machine (geometry 2)

The effects of air-gap length on the transient operation as well as on the synchronization process of the motor is also important. Figure 4.7 shows the transient speed and torque response of the motor. From figure 4.7(a) it can be seen that when air-gap length is decreased the synchronization become poorer. When air-gap

[1] Calculation of losses only include copper and iron loss

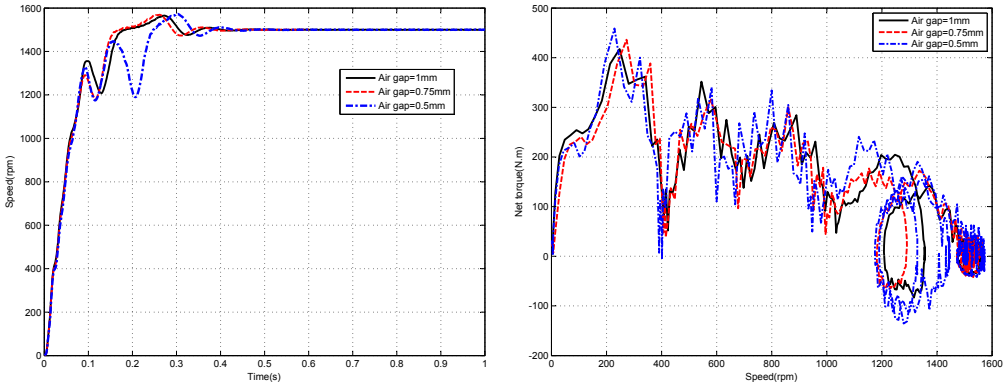

(a) Transient speed response

(b) Net torque vs Speed

Figure 4.7.: Transient response of reluctance motor with different air gap length

length is decreased the barking torque increased as can be seen from figure 4.7(b). Therefore, with the decrease in air-gap length the slip increased at the start of synchronization. Also from the figure 4.7(b) it can be seen that when air-gap length is decreased the synchronous torque increased. Therefore, decreasing air-gap length increases the braking torque and also the synchronous torque. Thus, there is a compromise between the torques while designing, as synchronization depends on both the torques.

4.2.4. Influence of magnet addition

The main disadvantage of reluctance motor is the poor power factor. In table 4.3 it can be seen that the power factor with air-gap length 0.5 mm is 0.79 which is lower compared to an induction motor or a PM motor. The power factor can be improved, as discussed in section 2.2.1, by increasing saliency of the rotor. The saliency can be increased either by increasing the d-axis inductance (L_d) or by decreasing q-axis inductance (L_q). Reduction in air-gap length increases L_d as explained in section 4.2.3. However, the air-gap length cannot be decreased after certain limit depending on the mechanical strength of the motor. The saliency can be increased further by reducing L_q which can be achieved by putting magnets in the motor. Now, to study the effect of magnets on L_q the magneto-static model of geometry 2 was simulated with different magnets volumes[2]. Figure 4.8 shows the arrangement of magnets in barriers. The magnets orientation was such that it opposed the flux from stator in the q direction.

It can be seen from the table 4.4 that by adding magnets the q-axis flux density was

[2]The volume of magnet is with respect to the volume of magnet used in the LSPM

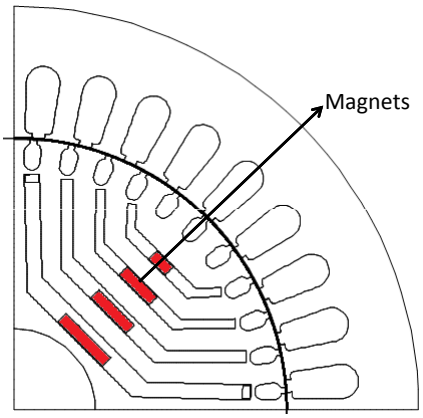

Figure 4.8.: Motor geometry with magnet placed in barriers

Magnet Volume (%)	Torque (N.m)	q-axis flux density(T)	d-axis flux density(T)	L_d/L_q
0.00	45.52	0.21	0.874	4.16
20.38	49.68	0.146	0.869	5.96
30.15	51.16	0.114	0.867	7.62
39.91	52.44	0.081	0.864	10.61
49.67	53.56	0.049	0.861	17.50
60.01	54.52	0.016	0.858	55.14
70.63	55.4	0.018	0.856	47.63

Table 4.4.: The d and q axis flux density at different magnet (NdFeB) volumes

reduced significantly. The small reduction in d-axis flux density is because of the saturation of iron due to the magnetic flux. As the reduction in q-qxis flux density is higher as compared to the d-axis flux density the saliency of the rotor increased with increase in magnet volume. The undesirable reduction in the d -axis flux density can be minimized by recalculating the insulation ratio such that saturation of iron is minimum. Moreover, the increase in saliency also increased the developed torque as given in the table. When saliency increases the difference in reactances of two axes also increases and hence increases the developed torque.

In tabel 4.4 it should also be observed that at 70% magnet volume the q-axis flux density is higher as compared to the flux density at 60% magnet volume. Increasing magnet volume more than 70% will further enhance the q-axis flux density and the motor will become like a PM motor. The effect of using Ferrite magnets was also calculated by replacing NdFeB magnets with Ferrite magnets and the results are given in table 4.5. The addition of Ferrite increased the saliency however, not as much as with NdFeB because of low remanent flux density of Ferrites. Comparing

tabel 4.4 and table 4.5 it can be seen that with 70% of Ferrite magnet or 30% of NdFeB magnet the motor has equal saliency.

Magnet Volume (%)	Torque (N.m)	q-axis flux density(T)	d-axis flux density(T)	L_d/L_q
0.00	45.53	0.210	0.874	4.161
20.38	47	0.189	0.874	4.675
30.15	47.76	0.178	0.874	4.986
39.91	48.4	0.167	0.874	5.340
49.67	49.2	0.157	0.873	5.749
60.01	49.6	0.146	0.873	6.249
70.63	50	0.134	0.872	6.845

Table 4.5.: The d and q axis flux density at different magnet(Ferrite) volumes

The magneto-static calculation does not account cross-magnetization in the motor. Thus, to obtain more accurate results transient simulation was done. Figure 4.9 shows the variation of power factor and efficiency with magnet volume. The power factor is increasing with the increase in magnet volume because saliency increases with magnet volume, discussed earlier. Another explanation of improvement in power factor is that the magnetic flux helps in reducing the magnetizing current drawn from the supply. The reduction in current also helps in improving the efficiency of the motor. The magnet addition also increases the developed torque and hence further reduces the line current required to deliver the load torque. Therefore, the efficiency of the motor also increased with the increase in magnet volume as shown in figure 4.9(a). It can also be observed from the figure that between 30% to 50% of magnet volume the rate of change of efficiency and power factor is low. Hence, the magnet use is not optimum in that range. Therefore, the design parameters like insulation ratio, stator coil turn number should be calculated accordingly, to optimize the use of magnets [14].

As discussed in section 2.1.1, the magnets cause braking torque in transient operation. Figure 4.10 shows the transient speed and torque response of geometry 2 with different magnet volumes. The motor is able to start and synchronize at rated load with and without magnets. However, as the magnet volume is increased the synchronizing process has become poorer. From the figure 4.10(a) it can be seen that increasing magnet volume increased slip at the start of the synchronization process. From the figure 4.10(b) it can be seen that adding magnet increased the synchronous torque and pulls the motor into synchronization despite high slip. The effect of increased braking torque got balanced by the increased synchronous torque. Therefore, magnets do not affect the synchronization of the motor very much however, significantly enhances the performance of the motor. Thus, reluctance motor with high efficiency and high power factor can be achieved by adding magnets.

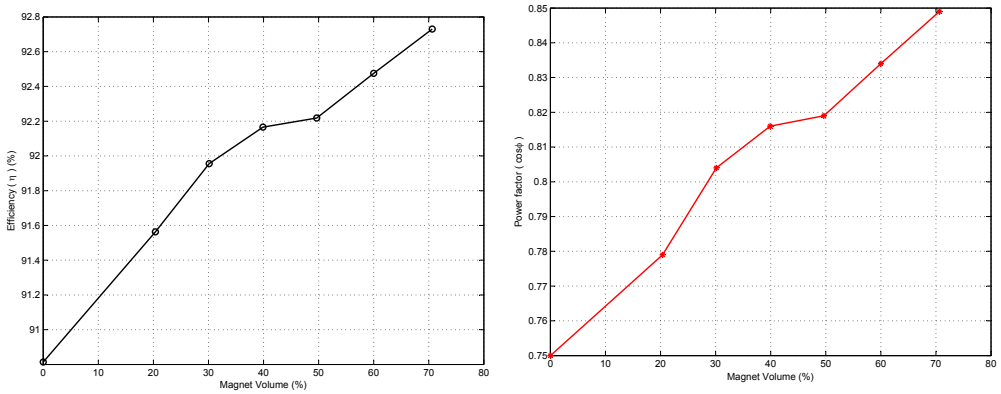

(a) Efficiency (η) (b) Power factor($cos\phi$)

Figure 4.9.: Variation in efficiency and power factor of geometry 2

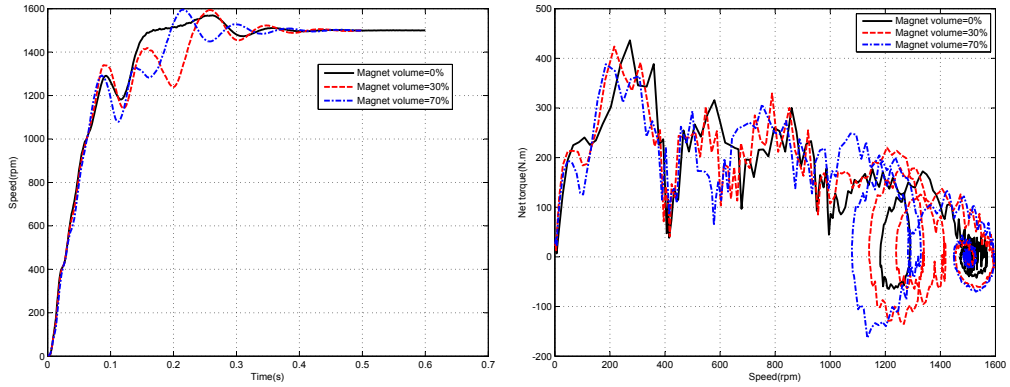

(a) Speed vs Time (b) Torque vs Speed

Figure 4.10.: Transient response of geometry 2 at rated load with different volumes of magnet

4.2.5. Length of Magnet

It is the length of magnet perpendicular to the magnetic flux lines that influence the performance of the motor, as shown in section 3.2.2. Therefore, better performance of the motor can be achieved by increasing the length of the magnet while magnet volume is same [15]. The effect of increased magnet length was studied using both the Ferrite and NdFeB magnets. The saliency of the rotor with increased magnet length at different magnet volume is shown in figure 4.11. When magnet length is increased the saliency of the motor has also increased marginally. Therefore, better performance can be achieved at same volume by increasing the length and reducing the width

of the magnet. However, as the increase in saliency is not large the reduction in magnet volume will not be large. Also magnets with lower width are more prone to demagnetization and hence limits the length of the magnet.

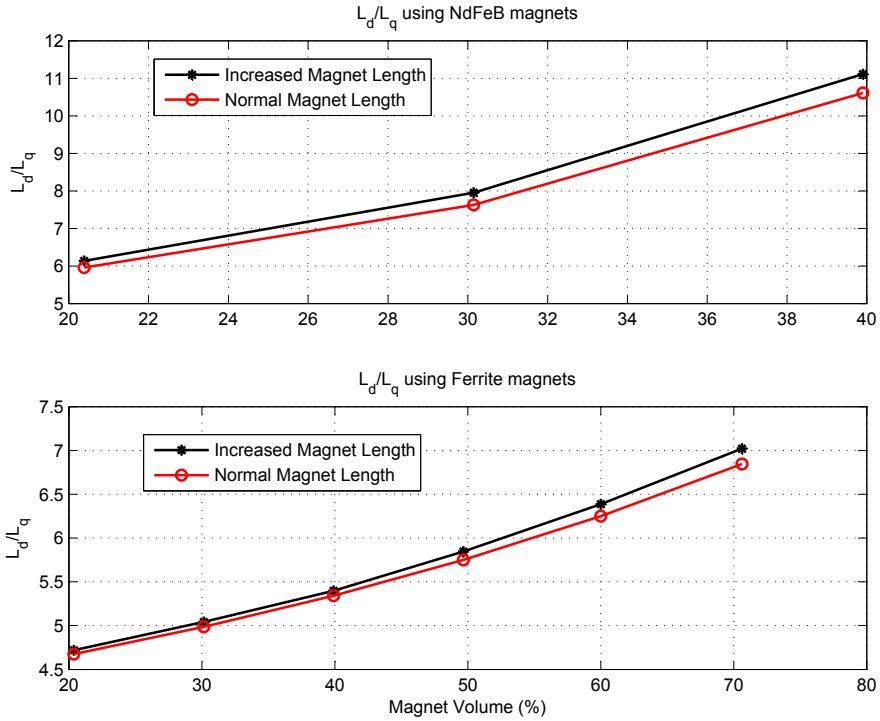

Figure 4.11.: Comparison of L_d/L_q of the rotor with increased and normal magnet length

4.2.6. Arrangement of Magnets

Unlike PM motors, the reluctance motor has more space for magnets due to more barriers. This increases the freedom to arrange magnets in the rotor. Figure 4.12 shows the cross section of the motor with four different arrangements of magnets. The total volume of the magnet was kept fixed to 40% of the magnet volume in LSPM. However, the magnet volume in different slots was changed by changing the length of the magnet. The thickness of the magnets in different slots was kept fixed. The performance of the motor with these arrangements is given in table 4.6.

As seen from table 4.6 the performance of motor varied with different magnet arrangements. The magnet arrangement shown in 4.12 (a) has highest saliency (L_d/L_q) as compared to other arrangements. However, the efficiency and power factor of 4.12(a) is lowest. In arrangement 4.12(a) the magnets are placed close to the air-gap which enhanced the opposition to stator field in the q direction due to magnets.

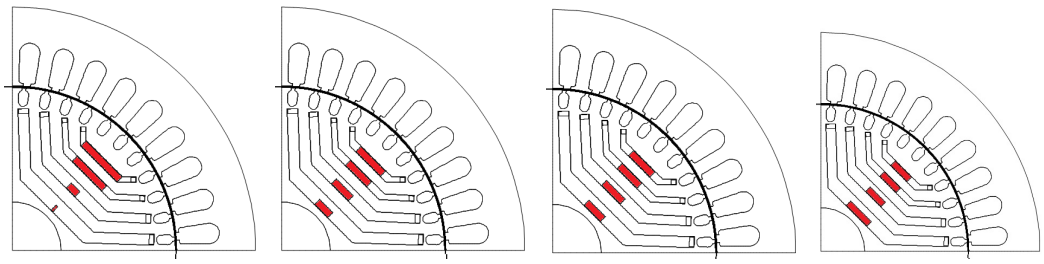

(a) (b) (c) (d)

Figure 4.12.: Same volume of magnet arranged differently in slots

Magnet arrangement	L_d/L_q	RMS Current (A)	Iron loss (W)	Efficiency (%)	Power factor $cos(\phi)$
a	13.82	25.2	156.80	91.45	0.79
b	12.29	23.9	142.68	92.23	0.82
c	11.92	23.7	140	92.36	0.83
d	11.43	23.7	138.40	92.36	0.83

Table 4.6.: Performance of motor with different magnet arrangements keeping magnet volume constant (40%), calculation of efficiency does not include stray loss

Therefore, the q-axis reluctance in arrangement 4.12(a) is lowest and thus highest saliency. However, the increase in saliency is not reflected in increase in the efficiency and the power factor. This is because the saliency of the rotor was calculated using magneto-static simulation which does not account cross-magnetization. The cross-magnetization can cause reduction in power factor as well as in efficiency [10]. Also as magnet is placed near to the air-gap it enhanced the air-gap flux density as well as harmonics and consequently increased the iron loss. Moreover, magnet concentration in one region causes saturation of iron which decreases the flux in the d direction. Thus, decreases the difference of reluctances and consequently the reluctance torque. Hence, the magnet arrangement 4.12(a) required maximum current to deliver the load torque. The increase in current due to less torque also caused more copper loss and thus lowered the efficiency. Also, putting magnets near to the air-gap makes it more prone to the permanent demagnetization.

From the table, it can be seen that the motor has highest efficiency and power factor when magnets are arranged as 4.12(c) and 4.12(d). In both the arrangements the magnets are evenly distributed and hence, caused minimum saturation of iron i.e. did not affect the d direction flux. Also more magnets are away from the air-gap which lowered the air-gap flux density as well as the harmonics and consequently lower the iron loss. The improvement in efficiency and power factor could be because of less cross-magnetization in these arrangements, as less cross-magnetization enhances the

saliency. Moreover, when magnets are placed away from the air-gap there will less chance of their demagnetization.

4.2.7. Stator coil turns

To optimize magnet the stator coil turn number should be selected properly. To study the effect of coil turn number geometry 2 was simulated with different coil turn number while magnet volume was kept fixed. The simulation results are given in table 4.7. It can be seen from the table, when turn number is increased the copper loss also increased and the iron loss reduced. Increasing turn number increases the back EMF and thus reduces the line current, whereas the total resistance of the coil increases. Thus, the net copper loss increased. It can also be seen from the table that when turn number is increased the power factor increased significantly. The inductance varies with the square of the turn number, thus increase in turn number increases the flux linkage. Therefore, increasing turn number reduces the magnetizing current drawn from the supply and hence, enhanced the power factor.

Number of turns	Iron loss (W)	Copper loss (W)	RMS Current (A)	Efficiency (%)	Power factor ($cos(\phi)$)
17	137.2	917.568	24.00	92.218	0.819
18	123.60	928.156	22.88	92.239	0.858
19	112.40	992.66	22.34	91.878	0.883

Table 4.7.: Effect of number of turns on motor performance

The asynchronous torque and pull out torque of a line start motor change drastically with stator coil turn number. Thus, affects both the starting and synchronization of the motor. Therefore, while deciding the turn number, the transient operation of the motor should be considered.

4.2.8. Effect of supply voltage

The supply voltage influence the synchronization of line start motor significantly. When supply voltage is reduced it affects the operation of the motor in two ways. Firstly, it lowers the asynchronous torque and thus reduces the acceleration at start. Therefore, the motor will have high slip at the start of synchronization. Secondly, it lowers the developed reluctance torque as reluctance torque varies with the square of the supply voltage. Thus, lowers the synchronous torque and consequently makes synchronization difficult. Geometry 2 was simulated with 10% under voltage with different magnet volumes. The transient speed response is shown in figure4.13. It can be seen that the motor with no magnet is not able to synchronize, whereas the

motor with 20% and 40% magnet volume synchronized. This is because the flux alignment torque is not very sensitive to supply voltage and hence increases the total synchronous torque. According to the results it seems that the motor should have atleast 40% of NdFeB magnet volume to be able to synchronize easily under low voltage.

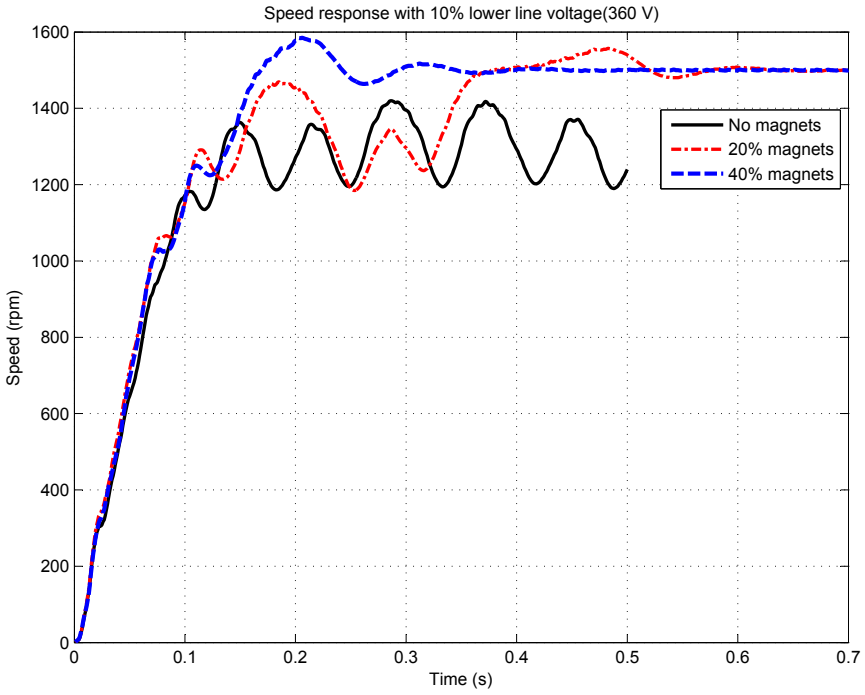

Figure 4.13.: Speed response geometry 2(air gap=0.5mm) with 360 V(line to line)

4.3. Proposed Design

The proposed motor is designed to meet two criteria firstly, efficiency of 91.4% and secondly, the power factor of atleast 0.86. Figure 4.14(b) shows the cross section of motor using NdFeB (Br is 1.14 and μ_r is 1.05 at 20^oC) magnet. The magnet volume in the motor is 40% as compared to the total magnet volume in LSPM. Figure 4.14(a) shows the design of the motor with Ferrite magnet (Br is 0.41 and μ_r is 1.35 at 20^oC). The volume of Ferrite magnet used is 107%. The stator and squirrel cage of the motor is same of the LSPM. The air-gap length of the motor is 0.5 mm.

Figure 4.15 shows the transient torque and speed behaviour of LSPM and the proposed motor (Line Start motor with high saliency). The speed response for both the motors is almost same. On comparing the starting torque it can be seen that

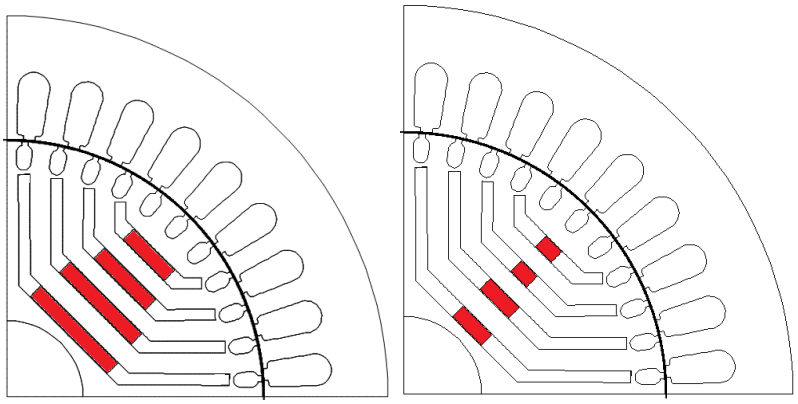

(a) Ferrite magnet 107% (b) NdFeB magnet 40%

Figure 4.14.: Cross Section of final design with 40% NdFeB and 107% of Ferrite magnet as compared to magnet volume used in LSPM motors

the proposed motor has higher torque at lower speed. However, at higher speed the LSPM has better torque. One reason could be that the LSPM has slightly higher synchronous torque than the proposed motor. This could be deduced from the fact that the efficiency of LSPM is slightly higher than proposed motor. Higher synchronous torque also implies higher braking torque. Hence, LSPM has slightly lower net torque than the proposed motor at lower speed. It can also be seen that the LSPM has better damping as compared to the proposed motor. The damping constant of the motor depends on the back EMF and the induced back EMF depend on the volume of magnet in motor [8].

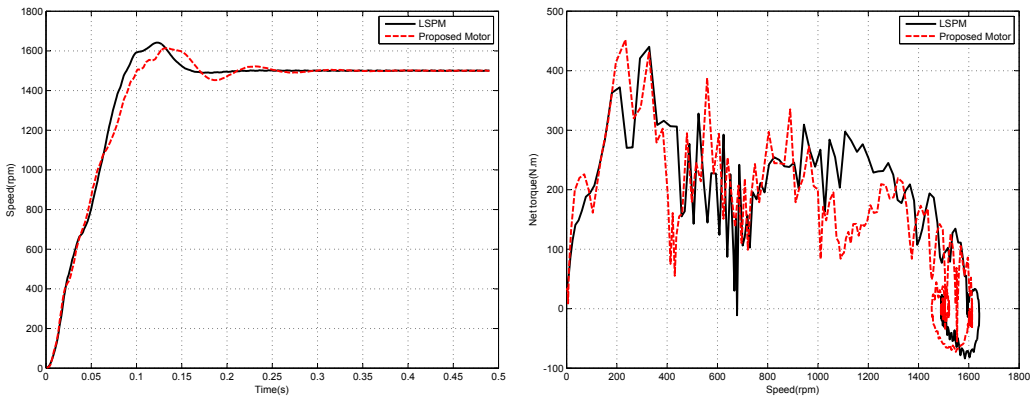

(a) Speed vs Time (b) Torque vs Speed

Figure 4.15.: Comparison between transient behaviour of LSPM and proposed motor (LSPM with high saliency)

The starting of LPSM also depends on the starting position of the rotor. The proposed motor was simulated with different rotor position at the start. Figure 4.16 shows the transient speed response of the motor with different rotor position. The speed response of the proposed motor is compared with the speed response of LSPM at same rotor positions. It can be seen that the speed response of both the motors are very close. Both the motors have same squirrel cage and hence have same asynchronous torque. Now, as the performance of both the motors differ slightly, the total synchronous torque will also differ slightly. This implies that there will be small difference in the breaking torque of the motors. From the results, it seems that the behaviour and performance of the motor depends on the total synchronous torque provided the squirrel cage and stator of the motors are same.

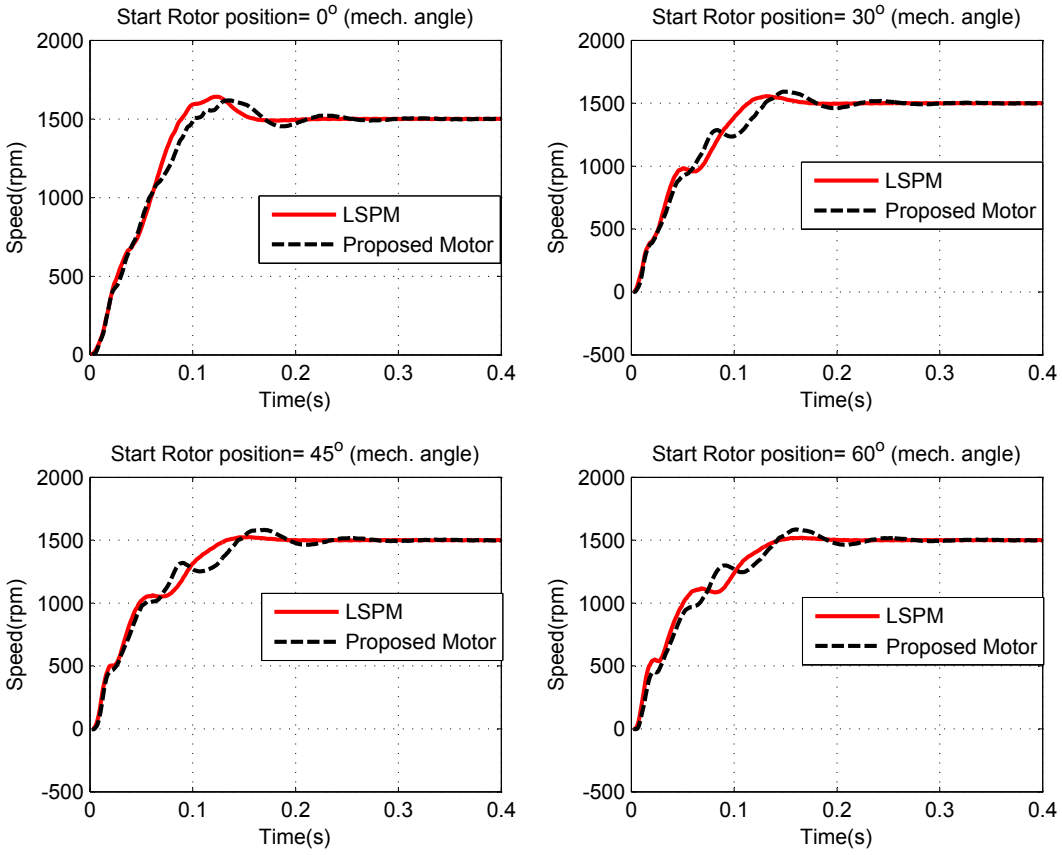

Figure 4.16.: Transient speed response of LSPM and the proposed motor at different rotor position at start

The performances of reluctance motor [3] (with NdFeB magnet and without magnet)

[3]The performance of reluctance motor is calculated using NdFeB magnets. Ferrite magnet can

and induction motor is given in table 4.8. The reluctance motors with air gap length 0.5 mm and 0.75 mm (with magnets and without magnets) are compared with induction motor with 0.75 mm air gap length. It can be seen that with the air-gap length 0.75 mm, the line current is almost same in both IM (Induction motor) and RM (Reluctance motor). When air-gap length is reduced to 0.5mm in the reluctance motor, the line current reduced to 25.2 A to deliver 12.5 kW output. The reduction in current reduced the copper loss as given in table 4.8.

The difference in iron loss of IM and RM (with air-gap 0.75) is 16 W. As iron is small portion of the total loss, the efficiency is not much influenced by the iron loss. The RM (with air-gap 0.75) has higher efficiency than induction motor. The higher efficiency of the RM is because of the no rotor loss and smaller stray loss compared to the IM. The calculation of stray loss is complicated and in this thesis work it was calculated using an software PPO 5 (used in XYLEM for designing of induction motor). In the software the stray losses are categorized depending on the source of stray load losses. The two components of stray loss depend on the stator current and rotor current. As there is not rotor current in the RM the stray loss is also lower than induction motor as given in the table. Therefore, synchronization of the motor helps in reducing stray loss. With the reduction in air-gap length of RM the stray loss increased however, the difference is not big. Reducing air-gap length caused reduction in the line current and consequently the stray loss also reduced. The increase in stray loss due to reduction in air gap length is somewhat compensated by reduction in stray loss due to line current. Therefore, the net total loss reduced and the efficiency increased with reduction in air-gap length.

From table 4.8 it can be seen that adding magnets in reluctance motor reduced the stray loss. The reduction in stray loss is due the reduction in line current. The effect of magnetic flux due to the magnets on stray loss is not considered in the calculation. Therefore, the calculation of stray loss might vary slightly with the magnets in the motor. The material used for lamination was M700-50A same as in LSPM. The efficiency of the motor improved by 0.33% (for 12.5 kW output motor) when the lamination was replaced with M470-50 A. The efficiency of the motor can be increased further by using higher grade of materials. The improvement in efficiency, when lamination was reduced, is because of reduction in iron loss. As iron loss is small part of total loss slight change does not bring significant improvement in efficiency. Table 4.9 gives the comparison of reluctance motor with induction motor with 11 kW output. The efficiency has improved if compared with the motors of 12.5 kW output. With 11 kW output, the line current reduced and hence the copper loss. Also as mentioned above, reduction in line current cause reduction in stray loss. The improvement in efficiency is also reflected in power factor of the motor.

replace NdFeB magnets.For example 107% of Ferrite magnets are required to match the performance of motor with 40% of NdFeB magnets and similarly 53% of Ferrite magnets are required to match with 20% of NdFeB magnets.

Motor Type	IM	RM		20%Magnet	40%Magnet
Air gap (mm)	0.75	0.75	0.5	0.5	0.5
Turns	17	17	17	17	17
Current (A)	26.4	26.6	25.2	23.3	22.1
Copper Loss (W)	1110	1128	996	865	778
Iron Loss (W)	120	136	139	140	140
Stray Loss (W)	400	242	266	239	225
Rotor Loss (W)	362	0	0	0	0
Frictional Loss (W)	44	44	44	44	44
Efficiency (%)	85.99	88.97	89.64	90.66	91.3
Power Factor	0.80	0.77	0.80	0.86	0.90
Pull out torque (N.m)	198	120	120	136	152

Table 4.8.: Summary of results for 12.5 kW Magnets used is NdFeB,IM=Induction motor,RM=Reluctance motor,Magnet % used is compared to LSPM

Motor Type	IM	RM	20%Magnet	40%Magnet
Air gap (mm)	0.75	0.5	0.5	0.5
Turns	17	17	17	17
Current (A)	24.4	21.8	21	19.9
Copper Loss (W)	948	757	703	631
Iron Loss (W)	122	139	140	140
Stray Loss (W)	329	197	186	177
Rotor Loss (W)	271	0	0	0
Frictional Loss (W)	44	44	44	44
Efficiency (%)	87.94	91.66	92.10	92.65
Power Factor	0.84	0.91	0.94	0.98
Pull out torque (N.m)	198	120	136	152

Table 4.9.: Summary of results for 11 kW Magnets used is NdFeB,IM=Induction motor,RM=Reluctance motor,Magnet % used is compared to LSPM

4.4. Summary

The magnet volume can be reduced if sufficient reluctance torque can be increased. As shown, in proposed motor 60% of the magnet can be reduced by increasing reluctance torque. The power factor of pure reluctance motor cannot match the power factor of a PM motors with same output. However, it could be improved by adding magnets. There is more space in rotor for magnets in reluctance motor as

compared to the LSPM. Hence, even more volume of cheap magnets can also be used to meet the requirement as proposed with 107% of Ferrite magnets. From the results obtained from the parametric study following things can be concluded for PM assisted line start reluctance motor (LSPM with high saliency).

- The synchronization of motor depends on the slip as well as the total synchronous torque of the motor. Therefore, the motor should have enough asynchronous torque to take to the right slip and sufficient synchronous torque to pull the motor in synchronization.
- In order to improve the performance of the motor it is better to increase the d axis inductance (L_d) rather than reducing q axis inductanceL_q at first. The reduction in air gap length improves L_d . Therefore, design should be improved by reducing air gap length to minimum. If the performance has to be improved further then L_q should be reduced by adding magnets or by flux barriers.
- The design should be optimized for corresponding volume of magnets. The insulation ratio, number stator coil turns and magnet arrangement in slots all vary with the magnet volume. Hence, the values of these parameters depend on the volume of magnet.
- The design of barrier is limited by the magnet size available. The barrier should not be too wide neither it should be very thin.

Chapter 5
5 Conclusion and Future Work

The thesis was focused on different methods to reduce the magnet volume used in LSPM. Three different methods to save magnet were studied. The magneto-static and transient model of the motor was used to simulate the operation of motor. The FEM software Flux 2D (by Cedrat) was used for simulations.

The influence of introducing flux barrier on flux density was calculated using magneto-static calculation. The flux barrier in LSPM reduced the leakage of magnetic flux. The calculated reduction in magnet volume is about 2%-3% of total volume. The iron ribs have significant affect on the magnetic flux leakage. Lower the thickness of iron-ribs better will be the air-gap flux density. However, manufacturing and mechanical constraints limits the thickness of iron-ribs.

The use of Ferrite magnets or SmCo along with the NdFeb in the motor was also studied. It was observed that replacing NdFeB magnets with SmCo did not affect change the flux density much. The price of SmCo is similar to NdFeB magnets and moreover, SmCo magnets are good for high temperature applications. However, the operating temperatures of water pumps are quite low. Hence, SmCo is not a very good choice to replace NdFeB magnets. The ferrite magnets can replace about 6%-7% of total NdFeB magnets volume without affecting the flux density. The use of two different magnets will become more effective if there will be some magnet material between the Ferrite and NdFeB (in terms of Energy product density). The choice of magnet also depends on the position of magnet in the rotor. In line start motor the magnet experience very strong demagnetizing field at the start of the motor. Hence, the intrinsic coercivity (H_c) of the magnet is more important than the operating temperature, in selection of magnets. The magneto-static simulation only calculates the influence of different magnets on flux density. The effects of using two grades of magnets on the steady state and transient state performance must be calculated using transient model. The calculated magnet volume reduction is marginal, hence further transient simulation was not done.

The design of LSPM with high saliency is studied. Both magneto-static and transient models were used to calculate the effects of saliency on the performance of the motor. At first, different aspects of the line start reluctance motor was studied. It was

found that it is better to align flux barriers with the rotor slots to produce maximum reluctance torque. It also implies that the numbers of flux barriers are limited by the number of rotor slots. The numbers of flux barriers and their width should be such that minimum saturation of iron happens. The air-gap length significantly influenced the performance of the motor. It was found that reducing air-gap length increased the reluctance torque as well the braking torque. The reduction in air-gap length enhanced the performance of the motor more than it deteriorated the synchronization process. It was observed that the calculated reluctance torque using magneto-static simulation was not varying much with the insulation ratio. However, the insulation ratio of the rotor should be such that the saturation of iron is minimized.

It was seen that the addition of magnet increased the saliency of the rotor and also enhanced the synchronous torque. On the other hand, increasing magnet volume also increased the braking torque and increased the slip (at the synchronization). However, it was found that despite high slip the motor synchronized because of high synchronous torque. Therefore, the magnets enhance the performance of motor. It was also observed that the motor with distributed magnets in barriers has better efficiency and power factor. Also keeping magnet in inner slots (away from air gap) decreases the demagnetization risk of the magnet. The stator coil turn number also affected the efficiency and power factor of motor. The asynchronous torque also depends on the turn number i.e. the acceleration of motor. Therefore, the turn number should be selected such that the motor starts as well as synchronize. It was found that under voltage made the synchronization of the motor difficult. The motor required at least 20% of the magnet volume to synchronize. Therefore, while designing LSPM with high saliency it is very important to consider the under voltage operation. All parameters affect the transient and the steady state operation in opposite way. Hence, in designing the LSPM with high saliency there is a compromise between the transient and steady state operation.

In the thesis two motor designs are proposed, one with 40% of NdFeB magnet volume and other with 107% Ferrite magnets. The volume of ferrite magnets required to achieve the desired performance is more. However, the cost of the magnet would be almost 10 times lower (at present ferrite cost). The proposed motor and LSPM has similar torque and speed response. Also the start of both the motors, at different rotor positions, were compared and found similar. The proposed motor was also compared with the induction motor of same rating. There is a big difference in total loss of the two motors. The proposed motor due to synchronous operation has no rotor loss. The stray loss in proposed motor is also lower as compared to induction motor. It was found that at lower output, the losses in proposed motor is even lesser which further improved the efficiency and power factor. One of the constraints in LSPM is that the rotor does not have enough space to place magnets. However, the proposed motor, because of many flux barriers, has enough space to place magnets. Therefore, with proposed design it is possible to achieve high performance motor using lower grade magnets like ferrite (as proposed in final design).

5.1. Future Work

In continuation to the thesis work it would be interesting to build the prototype and test them. Comparing simulation results with measurement would give better understanding of the working of motor. Some more work can be done in future are as follows :

- The proposed design of the motor is based on simulation results. The optimization of the parameters was done by hit and trial to achieve the required efficiency and power factor. Therefore, developing some analytical model will improve the understanding of parameters influence on the motor's performance and also on the transient state.
- The design of squirrel cage can be studied further to obtain better asynchronous torque for motor with flux barriers.
- The position of flux barriers are limited by rotor slots. It would be interesting to study the effect of asymmetric space between rotor slots on asynchronous torque. The result will also help in understanding the flexibility of barriers position mainly in d axis.
- The magnet is distributed in barrier slots and all parts of the motor does not have same magnetic condition (demagnetization filed or saturation).Hence, having different grades of magnet according to the condition can optimize the magnet cost further.
- The major part of loss is because of stator copper loss. To improve the efficiency of the motor redesign of stator can be studied further.
- The effect of magnet addition on the stray loss would make better understanding of losses in motor.

Appendix A

A Dimensional and performance details of LSPM

The motor optimized in the thesis work is LSPM, built at Xylem Water Solutions. The performance and constructional details of the LSPM motor is presented in this appendix. Figure A.1 shows a pole cross-section of the motor. As can be seen from the figure, the motor has 36 stator slots and 44 rotor slots. The magnet material used is NdFeB. The performance and dimensional details of the motor are given in table A.1

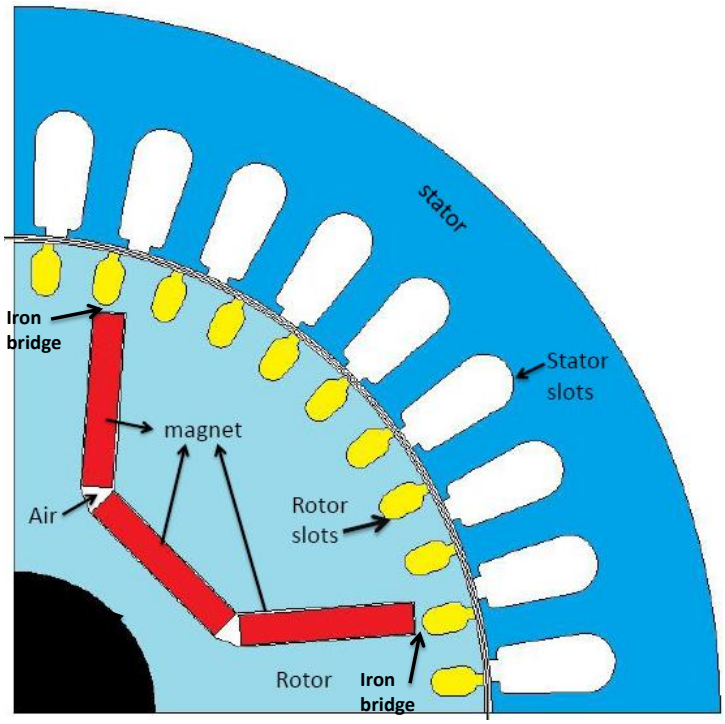

Figure A.1.: Cross section of a pole of LSPM

	Value	Unit
Number of phases	3	-
Number of poles	4	-
Number of stator slots	36	-
Number of rotor slots	44	-
Outer stator diameter	210	mm
Active length	180	mm
Shaft diameter	42	mm
Magnet material	NdFeB	-
Rated Current	18.93	A
Rated phase voltage (RMS)	230	V
Rated load	80	N.m
Rated speed	1500	rpm
Copper loss	571	W
Iron loss	190	W
Stray loss	225	W
Rotor loss	0	W
Frictional loss	44	W
Efficiency (%)	92.3	-
Power factor	0.98	-
Pull out torque	170	N.m

Table A.1.: Dimensional and Performance details of 12.5 kW LSPM

Bibliography

[1] NEOREM, "Personal communication: Nd and dy monthly average market prices in china (2012-06-14)."

[2] F. Libert, J. Soulard, and J. Engström, "Design of a 4-pole line start permanent magnet synchronous motor," in *Proceedings of the International Conference on Electrical Machines, ICEM 2002*, Brugge, Belgium, Aug. 2002.

[3] T. Miller, "Synchronization of line-start permanent-magnet ac motors," *IEEE Transaction on Power Apparatus and Systems*, vol. Vol. PAS-103, no. 7, July 1984.

[4] P. Niazi, "Permanent magnet assisted synchronous reluctance motor design and performance improvement," Ph.D. dissertation, Texas AM University, December 2005.

[5] U. Herslof, "Design analysis and verification of a line start permanent magnet synchronous motor," Ph.D. dissertation, KTH, 1996.

[6] S. Ruoho, "Modeling demganetization of sintered ndfeb magnet material in time-discretizaed finite element analysis," Ph.D. dissertation, Aalto University, 2011.

[7] A. Takahashi, S. Kikuchi, K. Miyata, S. Wakui, H. Mikami, K. Ide, and A. Binder, "Transient-torque analysis for line-starting permanent-magnet synchronous motors," in *Proceedings of the 2008 International Conference on Electrical Machines*. IEEE, 2008.

[8] J. Soulard and H.-P. Nee, "Study of the synchronization of line-start permanent magnet synchronous motors," *IEEE*, 2000.

[9] F. I. Ahmed, S. Abo-Shady, and K.F.Ali, "Synchronization of reluctance motors," *IEEE Transaction on Power Apparatus and Systems*, vol. Vol. PAS-100, no. 4, April 1981.

[10] M. Kamper and A. Volschenk, "Effect of rotor dimensions and cross magnetisation on ld and lq, inductances of reluctance synchronous machine with cageless flux barrier rotor," in *Proceedings of the Electr. Power Appl.*, vol. 141. IEE, July 1994.

[11] R. Vartanian, H. A. Toliyat, B. Akin, and R. Poley, "Power factor improvement of synchronous reluctance motors (synrm) using permanent magnets for drive size reduction," *IEEE*, 2012.

[12] R. R. Moghaddam, "Synchronous reluctance machine(synrm) design," Master's thesis, 2007.

[13] K. S. Khan, "Design of a permanent-magnet assisted synchronous reluctance machine for a plug-in hybrid electric vehicle," 2011.

[14] M. Barcaro, N. Bianchi, and F. Magnussen, "Permanent magnet optimization in permanent magnet assited synchronous reluctance motor for a wide constant power speed range," *IEEE*, January 2011.

[15] P. Guglielmi, B.Boazzo, E. Armando, G.Pellegrino, and A.Vagati, "Magnet minimization if ipm-pmasr motor design for wide speed range application," *IEEE*, 2011.

Declaration

I hereby certify that I have written this thesis independently and have only used the specified sources and resources indicated in the bibliography.

Stockhom , December 3, 2012

. . . . . .

Amit kumar jha